공학박사학위논문

Modeling and Analysis of Post-combustion and Pre-combustion CO_2 Capture Processes

연소 전 및 연소 후 이산화탄소 포집공정의 모델링 및 비교분석에 관한 연구

2016 년 2 월

서울대학교 대학원

화학생물공학부

정 영 수

Abstract

Modeling and Analysis of Post-combustion and Pre-combustion CO_2 Capture Processes

Yeong Su Jeong
School of Chemical & Biological Engineering
The Graduate School of Seoul National University

Climate change and its consequences have raised global awareness to reduce the anthropogenic emission of greenhouse gases, especially Carbon Dioxide (CO_2). Among the various sources of the CO_2 emission, power plants combusting fossil fuel such as coal, oil and gas occupy the most amount of CO_2 emission. Several methods of removing CO_2 from power plant flue gas have been proposed, and post-combustion and pre-combustion capture processes are most widely used candidates. Although post-combustion capture process is known as the most mature and economically feasible technology, its high energy consumption and efficiency penalty associated with process retrofit still remain as an obstacle towards commercialization. Pre-combustion capture process, on the other hand, has

higher efficiency than the conventional coal power plant and has no penalty associated with capturing CO_2. Although pre-combustion capture is more energy efficient and environmental-friendly, its high economic barrier still makes it difficult to be widely implemented.

In this study, both options of CO_2 capture process are modeled with reliable data source and analyzed technically and economically. For the post-combustion capture process, mechanical vapor recompression process is suggested as a solution to reduce the energy consumption to regenerate the absorbent. For the pre-combustion capture process, lean vapor compression, which is a widely used configuration for post-combustion capture, is also applied to reduce the steam consumption in the acid gas removal unit. As another application derived from the IGCC plant, substitute natural gas production process is also proposed which can produce a methane-rich product from coal.

Keywords: Carbon Capture and Storage (CCS), CO_2, MEA, Integrated Gasification Combined Cycle (IGCC), Substitute Natural Gas (SNG)

Student ID: 2010-31329

Contents

List of Figures

List of Tables

CHAPTER 1. Introduction

1.1. Research motivation

Among the OECD countries, South Korea has shown the highest carbon dioxide emission increase rate since 1990. In 2009, Korean government announced the CO_2 reduction target which corresponds to 30 percent of the total emission level in 2020 based on state of the art standards. Since then, tremendous efforts were made to reduce the CO_2 emission, and Carbon Capture and Storage (CCS) technology emerges as the most promising solution. Among several CO_2 capture technologies shown in Fig. 1-1, post-combustion technology has drawn much attention due to its applicability to large-scale CO_2 emission sources such as power plants or steel industries, and its suitability for retrofitting. Wet type capture of CO_2 requires the use of chemical absorbents, and amine-based solvents have been widely studied because it not only allows a large amount of CO_2 to be processed, but is also robust for a wide range of CO_2 concentrations. Although this approach in general is technically reliable since it had been successfully implemented in several chemical processes, the performance of solvent and the process itself still needs to be improved. [1] In the past, reducing the energy demand of CO_2 capture was achieved either by developing innovative absorbents with low

energy consumption or suggesting process alternative configurations which involve process or equipment retrofit.

Another popular CO_2 capture technology is pre-combustion, which can be represented by the Integrated Gasification Combined Cycle (IGCC) Plant. There are many environmental and performance benefits associated with application of IGCC technology. In addition to the generation efficiency, IGCC has less environmental emissions (SOx, NOx, PM and CO2) and solid waste generation in comparison with the Pulverized Coal (PC) Power Plant. [2] However, its cost requirement is very high compared to the conventional PC Power Plant. It is known that construction of a conventional PC power plant costs about $1,200/kW, whereas the estimated costs for building an IGCC plant can be as high as $2,000/kW, even in 2000 dollar standards. [3] In spite of the economic barrier of the IGCC plant, more plants are currently being planned and constructed worldwide.

Although it is very difficult to quantitatively determine which process has more competitive advantage, qualitative comparison between two processes in terms of performance and economics can be made by modeling approach.

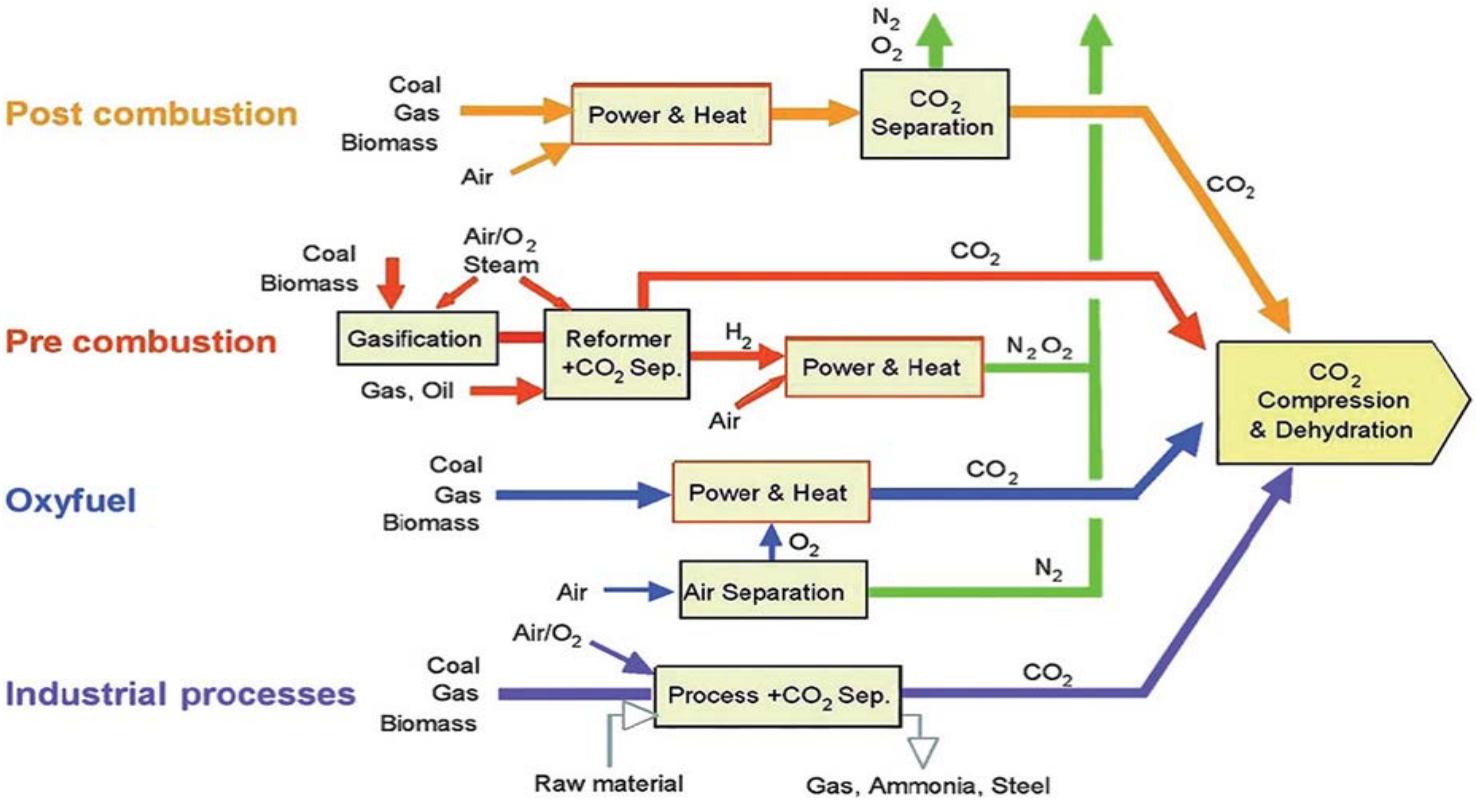

Fig. 1-1 Various technologies for CO_2 capture

1.2. Research objective

In this thesis, both options of CO_2 capture process are modeled and analyzed technically and economically. To ensure the validity of the models, post-combustion process is validated against the experimental data obtained from CO_2 capture facility, and pre-combustion process is modeled based on the technical report provided by well-known licensors. For the post-combustion capture process, mechanical vapor recompression process is suggested as a solution to reduce the energy consumption to regenerate the absorbent and an interface between capture and compression aspects of CCS value chain. For the pre-combustion capture process, lean vapor compression, which is a widely used configuration for post-combustion capture, is also implemented to reduce the steam consumption in the acid gas removal unit. As another application derived from the IGCC plant, substitute natural gas production process is also proposed which can produce a methane-rich product from coal. Final objective of this thesis is to qualitatively compare both CO_2 capture technologies to help develop decision criteria for selecting an appropriate process for CO_2 capture projects in the future.

1.3. Outline of the thesis

The thesis is organized as follows. Chapter 1 presents the motivation and objective of the research as introduction. Chapters 2 and 3 are dedicated to the post-combustion capture process where a model is developed using a commercial software and validated against real test bed data. Similarly, Chapters 4 focuses on model development of pre-combustion process with data provided from the licensor to ensure model's validity. Process alternative and another application similar to the IGCC plant is introduced in Chapter 5. Chapter 6 consists of the conclusion for this thesis and a brief remark on future work related to this study.

CHAPTER 2. Modeling of the Post-combustion CO_2 Capture Process*

2.1. Process overview

Post-combustion capture of CO_2 using aqueous amine-based absorbent is known as the most mature technology for commercialization. While most of the previous research can be categorized into two types: development of new absorbents or development of process alternatives, this study focuses on latter approach which captures CO_2 emitted from the conventional pulverized coal (PC) power plant. Data required for modeling and simulation are obtained from 0.1MW test bed facility located at Boryeong power plant in South Korea, which makes the entire disclosure of data somewhat difficult.

The advantages and disadvantages for post-combustion capture process are tabulated below.

Table 2-1. Advantages and disadvantages of chemical CO_2 absorption

Advantages	Disadvantages
- Technical maturity - Economic feasibility - Easy to scale-up - Retrofitablity	- High energy consumption for absorbent regeneration - Corrosion and thermal degradation of absorbent - Low CO_2 pressure

* Part of this chapter is taken from the author's published paper in the journal. [56]

MEA (Monoethanolamine) is the most conventional absorbent used in post-combustion capture process. It has been widely used in the acid gas removal process to remove H_2S and CO_2 from the crude gas. [4] In spite of its capture effectiveness, thermal energy required for absorbent regeneration remains as an obstacle, because the primary energy source is steam extracted from the power plant.

2.2. Process modeling and simulation

With courtesy of KEPCO E&C Company, operation data from the 0.1 MW CO_2 capture test bed unit at Boryeong power plant were obtained, treating approximately 350 Nm^3/hr of flue gas containing 10-15 volume % of CO_2. Construction of this facility was completed in 2010 and it can recover two tons of CO_2 emitted from pulverized coal-fired Boryeong power plant #7 and #8, each with 500 MW of electricity generation capacity. Overview picture of the facility and process schematics are shown in Fig. 2-1. This post-combustion amine capture process configuration is conventional and similar to other CO_2 capture projects worldwide. Compression facility was also added to the CO_2 capture test bed in 2013, and it was designed to compress approximately 25% of CO_2 captured from the test bed. The process mainly includes a compressor package, dryer package for dehydration, and chiller package for CO_2 liquefaction. Liquefied CO_2 at 20 bar is temporarily

stored in a vessel and then passes through an ambient evaporator before being sent back to the stack.

Using the data collected from the test bed campaign in 2011, CO_2 capture process using Monoethanolamine (MEA) solvent was modeled and validated using Aspen Plus (V7.3) with RateSep™ package, which can simulate the behavior of non-ideal reactive distillation systems appropriately. [5]

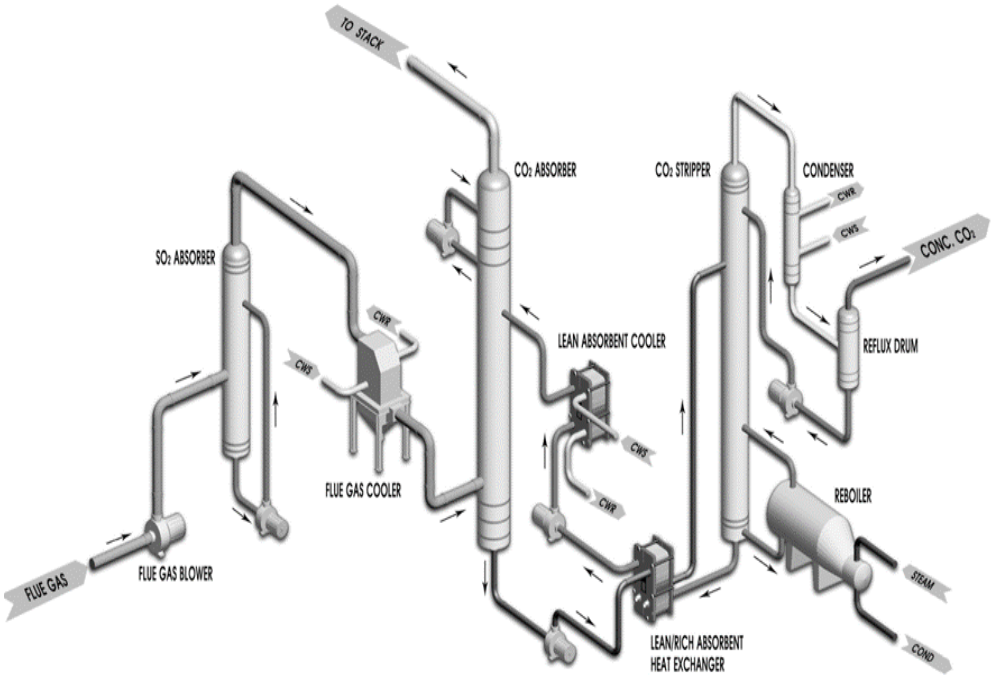

Fig. 2-1 Process schematics of 0.1MW Test Bed in Boryeong, South Korea

2.2.1. Thermodynamic model

From previous simulation approaches of CO_2 capture process, a vapor–liquid-equilibrium (VLE) model based on the activity coefficients model, electrolyte non-random two-liquids (ElecNRTL), was the most apparent selection for describing CO_2–H_2O–MEA systems. [5, 6] This property method takes into account for the Hillard thermodynamic representation, reaction kinetics of CO_2 with MEA solution, and various heat and mass transfer phenomena associated with this system of mixture.

Among the constituents of the flue gas, light gases such as N_2, CO_2 and O_2 were selected as Henry components and Henry's constants of these components were specified with water and MEA, respectively. Table 2-1 shows Henry's constant parameters for the light gases, and Henry's constants can simply be calculated using Eq. (2-1) with parameters given in the table. The parameters of CO_2 in H_2O were obtained from the vapor liquid equilibrium (VLE) data of Takenouchi et al. [7], Dodds et al. [8], and Drummond[9], and those in the MEA were regressed based on the work of Wang et al. [10].

$$\ln H_i^{Po} = C_1 + \frac{C_2}{T} + C_3 lnT + C_4 T \qquad (2\text{-}1)$$

Table 2-2 Henry's constant parameters of light gases

Henry's Component	**CO_2**	**CO_2**	**N_2**	**O_2**
Solvent	**H_2O**	**MEA**	**H_2O**	**H_2O**
Temperature units	K	K	K	K
a_{ij}	-145.316134	20.176	176.507	155.921
b_{ij}	765.888228	-1139	-8432.77	-7775.06
c_{ij}	32.2472704	0	-21.558	-18.3974
d_{ij}	-0.07395071	0	-0.008436	-9.44E-03

Seven reaction models are involved in this study to describe the chemical reactions in the absorber and stripper columns. The power law expression is used for chemical reaction model. All reactions are assumed to be in chemical equilibrium except those of CO_2 with OH- and CO_2 with MEA. From Eqs. (2-2) to (2-6), the equilibrium constants were calculated from the change in standard Gibbs free energy. The equilibrium constants for Eqs. (2-7) and (2-8) were obtained from the work of Austgen et al. [11], and the kinetic parameters of these reactions were taken from Hikita et al. [12]

$$H_2O + MEAH^+ \leftrightarrow MEA + H_3O^+ \quad (2\text{-}2)$$

$$2H_2O \leftrightarrow H_3O^+ + OH^- \quad (2\text{-}3)$$

$$HCO_3^- + H_2O \leftrightarrow {CO_2}^{2-} + H_3O^+ \quad (2\text{-}4)$$

$$CO_2 + OH^- \leftrightarrow HCO_3^- \quad (2\text{-}5)$$

$$HCO_3^- \leftrightarrow CO_2 + OH^- \quad (2\text{-}6)$$

$$MEA + CO_2 + H_2O \leftrightarrow MEACOO^- + H_3O^+ \quad (2\text{-}7)$$

$$MEACOO^- + H_3O^+ \leftrightarrow MEA + CO_2 + H_2O \quad (2\text{-}8)$$

2.2.2. Flowsheet description

Aspen flowsheet of the capture process is shown in Fig. 2-2. The flue gas from the power plant first enters the direct contact cooler (AB-101) where sulfur derivative residues are removed before being introduced to the absorber (AB-201), which is operated near ambient pressure. The flue gas in the absorber flows counter currently with the MEA solvent from the top and chemically reacts with the solvent. This CO_2 absorption reaction is an exothermic reaction which also accompanies multicomponent mass and heat transfer in an absorption column [13]. The CO_2 lean stream is then partially condensed in the washing zone (HE-206) to recover water and the absorbent, and remaining CO_2 lean flue gas is vent through stack. In the stripper column (SV-201), CO_2 is thermally detached from CO_2-rich MEA solvent using the steam extracted from power plant. A fin-and-plate type lean and rich amine heat exchanger (HE-202) between two columns is designed with a specific minimum temperature approach (MTA) value; however, it was very difficult to control the MTA in the actual experiment, so the temperature of the rich amine stream leaving the cold side of the heat exchanger was set to a fixed value of 93^{o}C before entering the stripper column. Regenerated lean amine stream from the stripper flows back to absorber via HE-202 in order to complete the circulation loop.

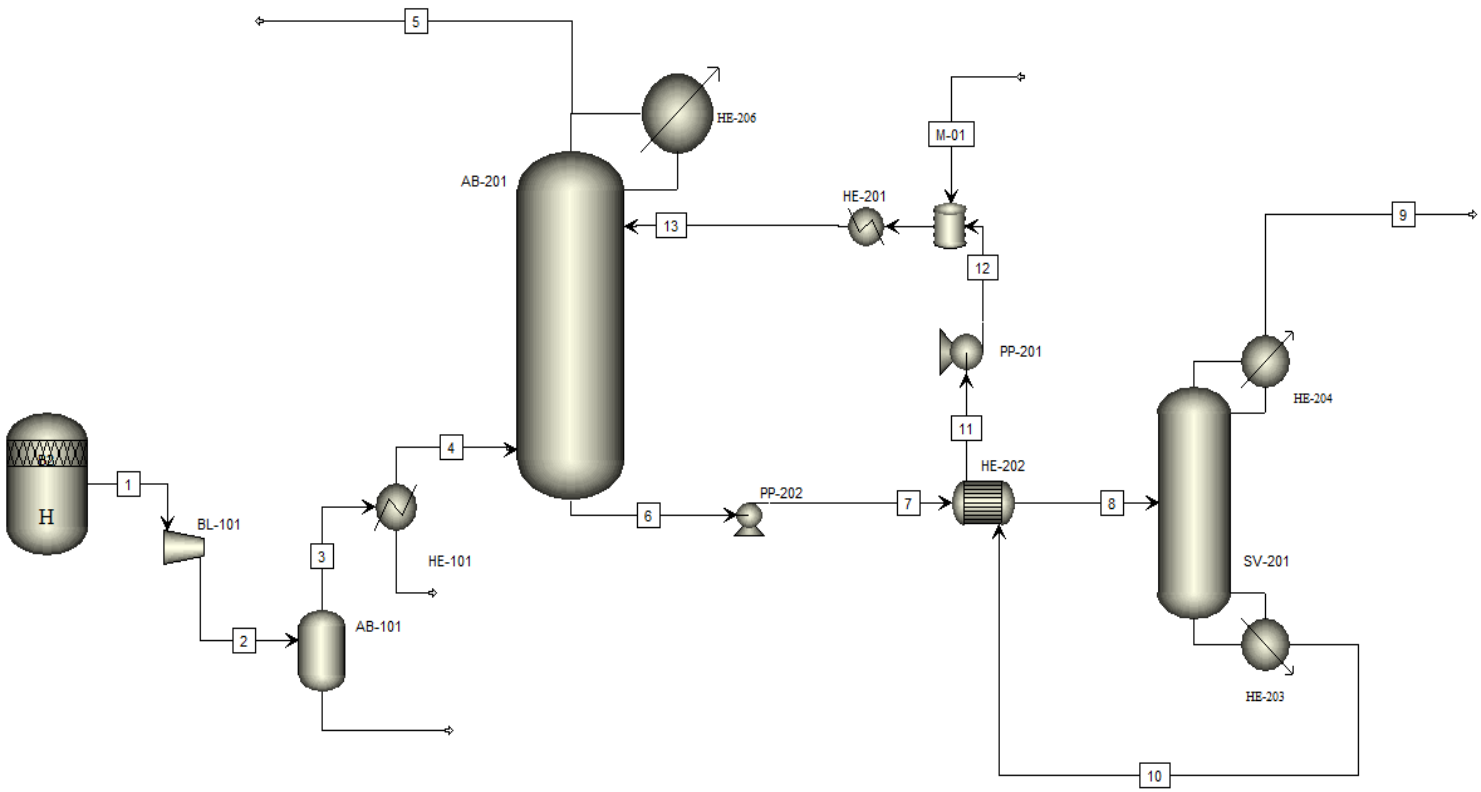

Fig. 2-2 Aspen Plus flowsheet of the post-combustion CO_2 capture process model

Table 2-3. Conditions of flue gas and absorbent

Items	Value	Unit
Flue gas temperature	48.1	℃
Flue gas Pressure	1	atm
Flue gas flow rate	350	Nm^3/h
Lean MEA temperature	40	℃
Lean MEA flow rate	1,235	L/hr
Lean MEA loading	0.26	
Flue gas composition (mole fraction)		
N_2	0.718	
CO_2	0.132	
H_2O	0.112	
O_2	0.038	

2.3. Process validation

While performance of post-combustion CO_2 capture process is basically evaluated by the amount of reboiler's heat duty for solvent regeneration, performance of our model is evaluated by comparing temperature profiles within each column, which has six and five thermocouples, respectively. Since parameters primarily affecting the shape of internal temperature profile are related with heat and mass transfer phenomena within the column, interfacial area and heat transfer factor values were varied to match the temperature profiles. Increasing the interfacial area factor directly increases the heat transfer rate whereas increasing heat transfer factor has no apparent impact on mass transfer rates [14]. Film discretization is also considered for film reactions between liquid and vapor interface. The absorber model uses 16.8 m of random packing (IMTP#25) with HanleyIMTP mass transfer correlation [15] and Chilton-and-Colburn heat transfer correlation. Countercurrent flow model is used to calculate bulk properties in mass and energy fluxes, and a total of 6 film discretization points were specified for film reactions. The stripper model uses 11.75 m of same packing type as well as the same mass and heat transfer correlation, but film discretization was not added and Vplug flow model was used instead to better match the temperature profile. Validation of the model was

accomplished by minimizing the difference between simulation results and operation data for the both columns, and the results are shown in Fig. 2-3. Simulation model predicts both profiles precisely, which uses interfacial area factor of 1.2 and mass transfer area factor of 0.6.

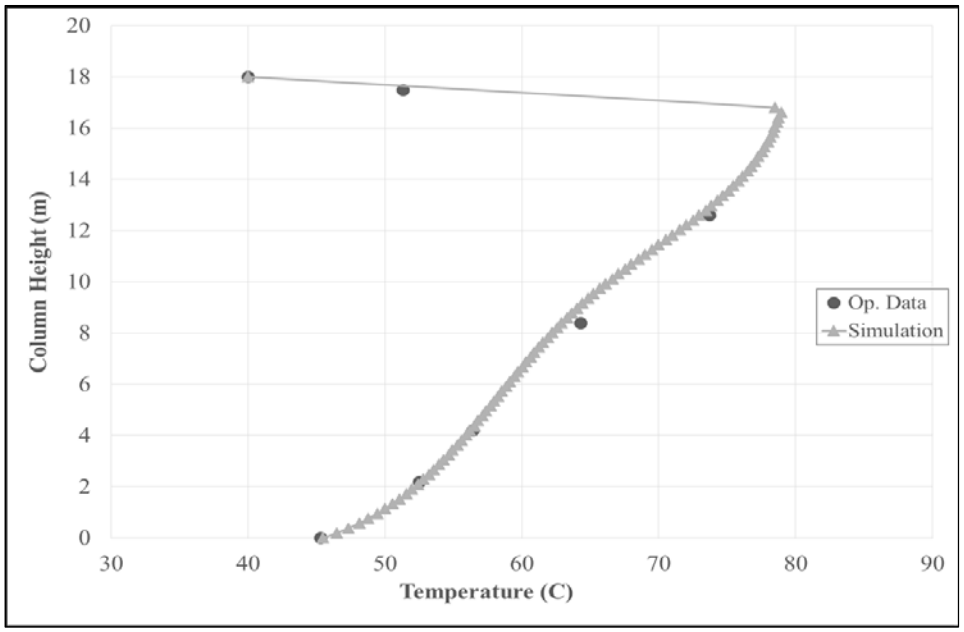

(a) CO_2 capture process absorber temperature profile

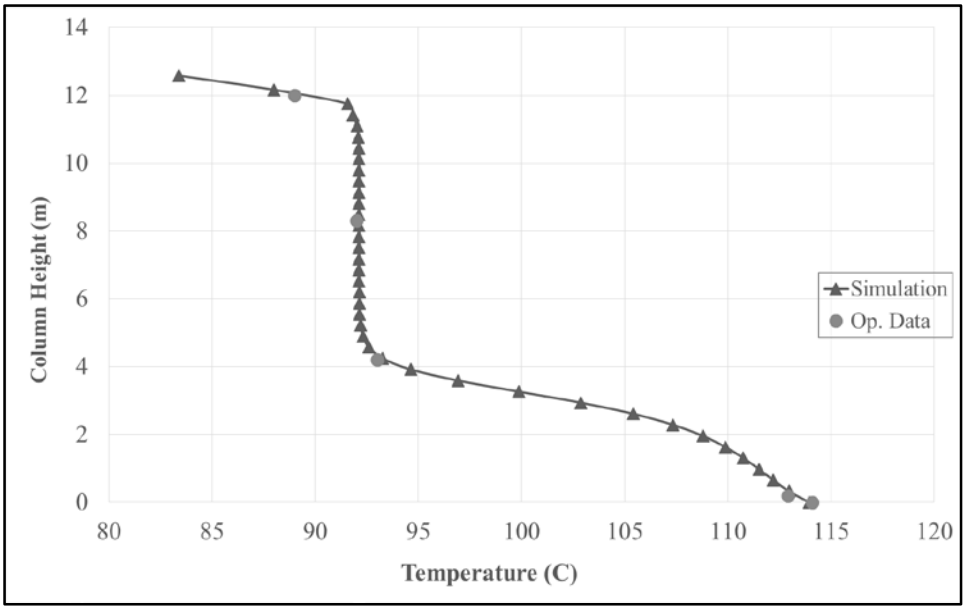

(b) CO_2 capture process stripper temperature profile

Fig. 2-3 CO_2 capture process column temperature profiles [16]

2.4. Results and discussion

First, exergy analysis on the CO_2 capture process was performed to determine which unit contributes to the most exergy loss the most. Fig. 2-4 shows the exergy loss of the unit operations in the post-combustion CO_2 capture process. Apparently, two columns and the main heat exchanger are responsible for about 85 % of the total exergy loss.

Several improvements can be implemented to reduce both energy consumption and exergy loss of the process. In the base case, the temperature of the rich amine steam exiting the HE-202 was fixed at 93^{o}C, in order to prevent cavitation effect in the heat exchanger. The exergy loss of the stripper can be reduced by implementing advanced process configurations such as heat exchanger network or vapor recompression. In this thesis, mechanical vapor recompression process is considered to reduce the amount of exergy destruction as well as the amount of steam consumption in the stripper. Process details, modeling procedure and simulation results are presented in Chapter 3.

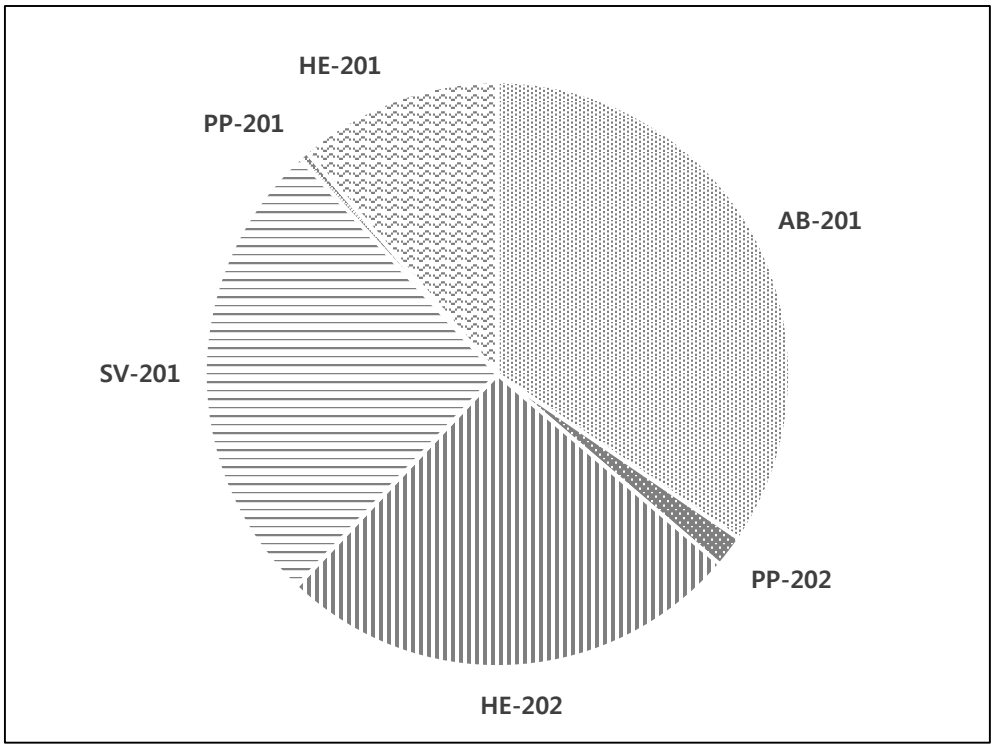

Fig. 2-4 Exergy loss of the unit operations in CO_2 capture process

CHAPTER 3. Analysis of the Post-combustion CO_2 Capture Process[†]

3.1. Overview

In this chapter, post-combustion CO_2 capture process model is modified in order to enhance the process efficiency. Because the solvent regeneration step in the CO_2 capture processes consume a significant amount of energy, the process modification is essentially focused on retrofit of stripper configuration, which is directly related to the thermal energy consumption. Thermal energy consumption for absorbent regeneration in the stripper column still remains as the biggest challenge to overcome for amine-based absorbents.

Absorbent regeneration is achieved by thermal energy provided by steam extracted from the power plant. As shown in Fig. 3-1, steam could be extracted from various locations from the turbines, it is most common to extract steam from IP/LP crossover (D) or the first LP steam turbine (E). Apparently, extraction of steam leads to de-rate of electricity generation efficiency, up to about 30%.[18, 19] This de-rate effect makes it even more important to reduce the thermal energy requirement for absorbent regeneration, especially for the MEA solvent.

[†] Part of this chapter is taken from the author's published paper in the journal. [56]

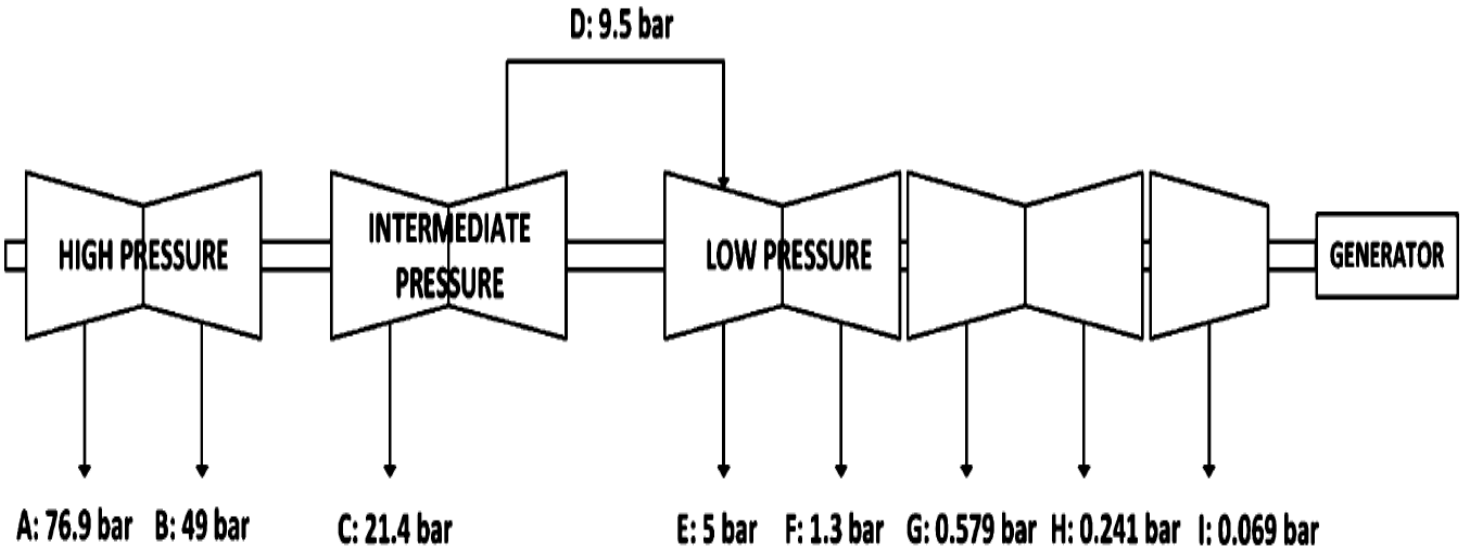

Fig. 3-1 Possible steam extract locations from power plant [17]

3.2. Mechanical Vapor Recompression (MVR) process

3.2.1. Process description

The concept of a MVR process has been widely implemented in other chemical processes such as seawater desalination or waste water treatment systems. [20, 21] This process converts electrical energy to thermal energy to reduce the steam consumption in the reboiler, which means less de-rate effect in power plants' electricity generation efficiency. Applying a MVR process to the post-combustion CO_2 process can also produce CO_2 at higher pressure so that the energy consumption for CO_2 compression can also be reduced. The condenser required for the stripper column is eliminated and saturated vapor leaving the top of column is fed directly into the first stage of compressor chain instead. As shown in Table 3-1, the overhead vapor steam of the stripper contains approximately 50 mol% of water, and the latent heat of water can be recovered by compressing the overhead vapor stream and exchanging heat with reboiler, reducing the thermal energy required for solvent regeneration. Although the overhead vapor stream has a lower temperature than that of reboiler, saturation temperature of the vapor stream increases as the pressure increases, allowing both sensible and latent heat of the steam in the overhead stream to be recovered as the heat source of the reboiler.

Table 3-1. Stripper overhead stream information for MVR process

Stream Composition	Value	Unit
CO_2	48.9	mol %
H_2O	51.1	mol %
MEA	Trace	mol %

Fig. 3-2 shows the process flow diagram for the MVR process. For this process, two-stage compression with the same compression ratio was assumed, and the temperature approach of 5 K between a multi-stream heat exchanger and reboiler was assumed. The final product of MVR process will be CO_2 gas at 20 bar, which can be directly liquefied for ship or pipeline transport. Sensible heat from superheated region as well as the latent heat of the condensed water vapor can be recovered from the intercooler between compression stage, and water drawn from each stage is collected and sent back to the stripper as reflux. The amount of latent heat recovered is determined by operating pressure of the stripper which determines the temperature of the reboiler, and the temperature approach set between heat exchanger and the reboiler.

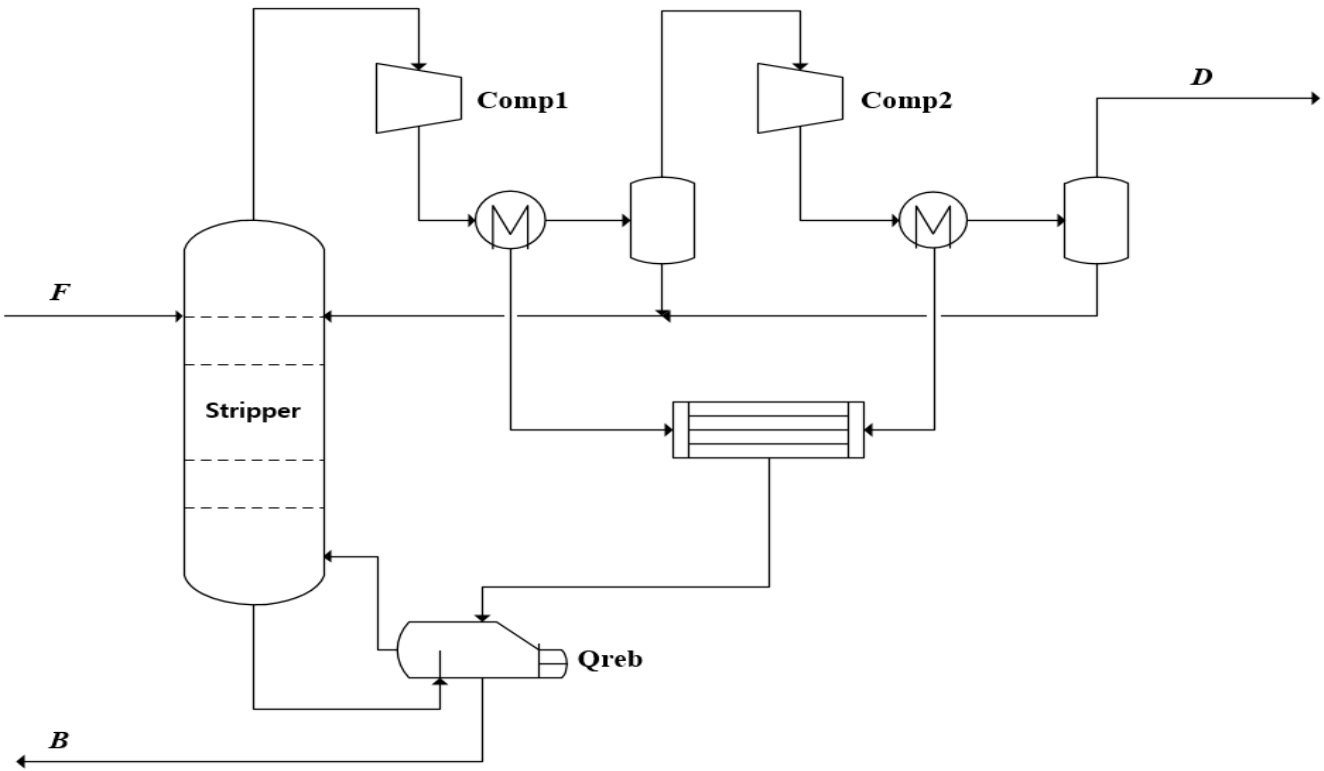

Fig. 3-2 Process schematics of MVR configuration for stripper

3.2.2. Simulation results

The total energy consumption is very important to obtain technical and economic feasibility of the CO_2 capture project. Although the regeneration energy for the capture process is fixed for a specific stripper operating pressure, the additional energy for compression as well as the amount of latent heat recovered from the MVR process can be optimized. The total amount of compression energy depends on the inlet pressure of the MVR compressor, which is equivalent to the operating pressure of the stripper column.

From the base case scenario, thermal energy consumption for solvent regeneration is 3.42 GJ/ton CO_2 captured and compression energy consumption is 0.28 GJ/ton CO_2 captured (6.6 kW). Applying the electricity to thermal energy conversion factor of turbine efficiency, energy consumption of the compression process corresponds to 0.60 GJ/ton CO_2, adding to the total energy consumption of 4.02 GJ/ton CO_2. Additional energy required for liquefaction was not considered to make an appropriate comparison with the MVR model. MVR process at 1.5 bar inlet pressure has total energy consumption of 3.69 GJ/ton CO_2, which corresponds to 8.2% reduction in total energy consumption compared to the base case scenario. MVR process at 1.8 bar showed similar saving effects in comparison with the base case. Summary of simulation results are shown in Table 3-2.

Table 3-2. Simulation results of the MVR process

	Unit	Base Case	MVR (1.5bar)	MVR (1.8bar)
Absorbent regeneration energy	GJ/ton CO_2	3.42	2.80	2.86
Heat recovered from compression	kJ/hr	-	50.66	37.51
Electrical energy consumption	kW	6.60	9.56	8.80
Total energy consumption	GJ/ton CO_2	4.02	3.69	3.68
Energy saving effect	%	-	8.22	8.43

3.2.3. Technical analysis

From the simulation results, a trade-off relationship was observed between the amount of heat recovered and electrical energy consumption. As electrical energy consumption increases, the amount of heat recovery also increases. In order to find better operating condition for MVR process, exergy analysis were performed. When assessing the performance of a chemical process, energetic performance based on the first law of thermodynamics, which includes electric power consumption and thermal efficiency, is generally used. However, in recent years, the exergetic performance based on the second law of thermodynamics is also emerging as a useful method in evaluation and optimization of various processes. [22, 23] In this thesis, exergy analysis for the stripper column was performed to determine optimal operating condition for the MVR process. First, the system boundary for the base case was defined as shown in Fig. 3-3. Then, the intrinsic amount of destroyed exergy (also referred to as irreversibility) in the stripper column can be quantified by appropriate exergy balance which can be written as equations (1) through (3) shown below. Reference temperature value was assumed at 300 K, and the temperature of steam and cooling water were taken from design data from the test bed.

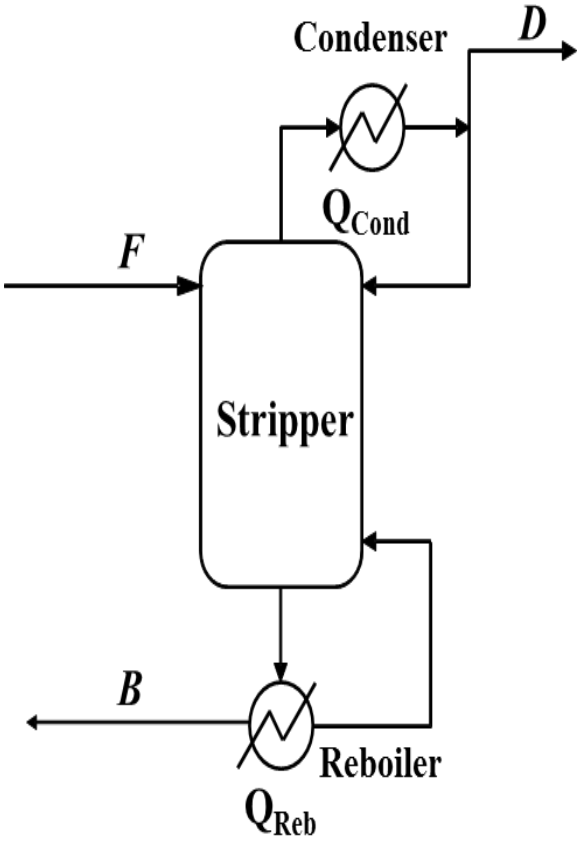

Fig. 3-3 System boundary for exergy analysis in the stripper column

$$\dot{I} = \sum \dot{E}_{in} - \sum \dot{E}_{out} + \sum \dot{E}_Q - \sum \dot{E}_W \quad (3\text{-}1)$$

$$\mathrm{E}_i = \dot{m}_i[(h_i - h_0) - T_0(s_i - s_0)] \quad (3\text{-}2)$$

$$\sum \dot{E}_Q = Q_{Reb}\left(1 - \frac{T_{Reb}}{T_{Steam}}\right) + Q_{Cond}\left(1 - \frac{T_{CW}}{T_{Cond}}\right) \quad (3\text{-}3)$$

$$\sum \dot{E}_W = 0$$

$$T_0 = 300K;\ T_{CW} = 303K;\ T_{STEAM} = 420.5K$$

A similar balance was written for the MVR case, except for the work term. Additional compressor work must be taken into account, which will reduce the amount of destroyed exergy from the column. For a two-stage compression system, the work term can be written as shown in equation 4 below.

$$\sum \dot{E}_W = T_0(s_i - s_0)_{comp1} + T_0(s_i - s_0)_{comp2} \quad (3\text{-}4)$$

The amount of exergy destruction for the base case, MVR starting at 1.5 and 1.8 bar are shown in Fig. 3-4. The figure shows that MVR at 1.5 bar has the least amount of exergy destroyed, mainly caused by the difference in the heating duty of the reboiler.

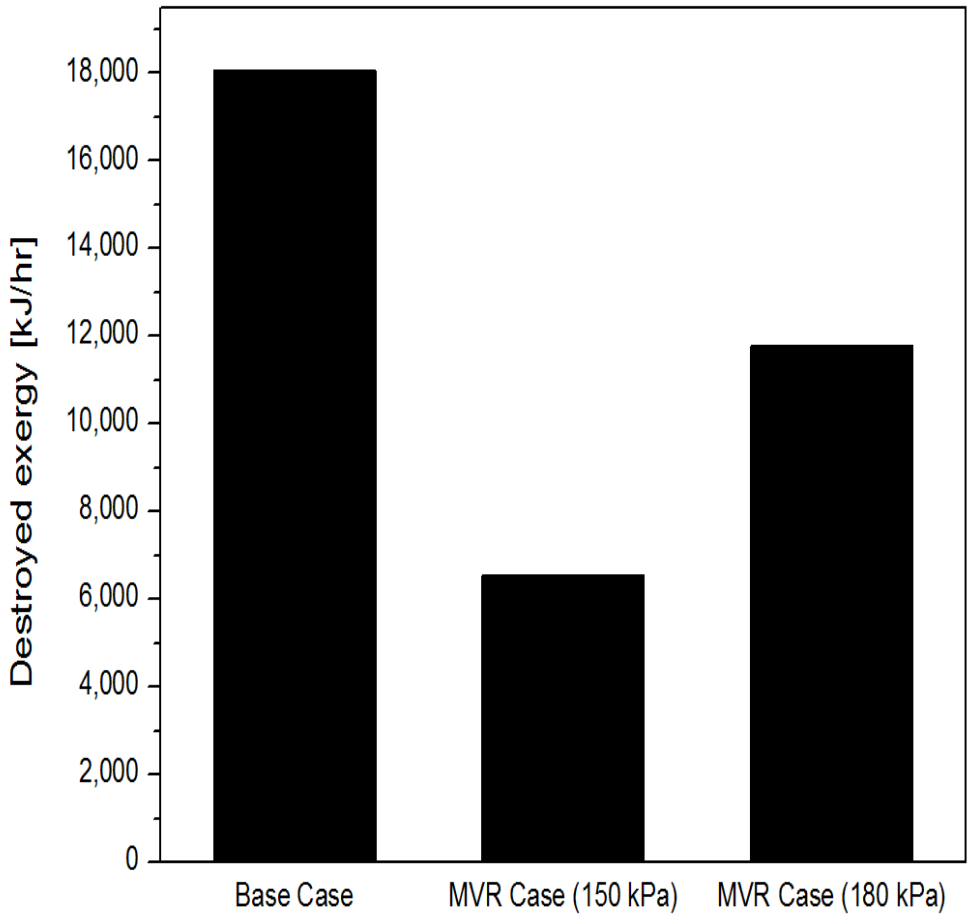

Fig. 3-4 Total amount of destroyed exergy for the stripper column

3.2.4. Economic analysis

Less amount of exergy destruction does not always guarantee optimum operating condition for the process. In particular, to apply MVR process for CO_2 capture, economic factors such as costs of additional equipments or costs of electricity must be considered. Information on capital and operating costs were gathered from literature and several assumptions were made. [24-26] Economic depreciation was assumed to be 5% over 30 years. [27] Cost of cooling water and LP steam was assumed as \$0.013/m^3 and \$5.5/ton, respectively. [28] Also, the price of electricity, \$0.065/kWh, was assumed based on a 2010 U.S. Department of Energy report. [29] Electricity price for industrial use is much lower in Korea, but the U.S. value was used to have less contingency in cost estimation. Costs of installed equipment were calculated by Aspen Process Economic Analyzer (V7.3) and the procedure for estimating both capital investment and operating expenditure was taken from Peters. [26] A brief summary of installed process equipment costs calculated from Aspen Process Economic Analyzer is shown in Table 3-3.

As can be seen from the cost breakdown, the CO_2 compressor unit takes up the largest portion of the equipment costs, and the cost increases for the MVR scenario result from the increased compressor work. The scenario where the MVR operates at 1.8 bar has the lowest equipment costs, because

the condenser in the stripper column is eliminated and the compressor work is less than in the 1.5 bar scenario. To make an appropriate comparison among each scenario, capital costs were annualized by calculating the equivalent annual cost (EAC) by equation (5) below.

$$EAC = \frac{NPV}{A_{t,r}},\ where\ A_{t,r} = \frac{1-\frac{1}{(1+r)^t}}{r} \qquad (3\text{-}5)$$

Peters' method uses a wide range of values for estimating each category for the economic evaluation. For the capital costs, values were assumed so that the ratio of direct to indirect costs is 80:20, and for the operating costs, average values were assumed for each category. In calculating the operating costs, the amount of utility consumption such as cooling water, LP steam or electricity was directly taken from simulation data. Annualized costs for the base case and two of the MVR scenarios are shown in Fig. 3-5, and it can be seen that the MVR process at 1.8 bar scenario has the lowest costs associated with the system. The detailed summary of capital and operating costs for each scenario is shown below in Tables 3-4 and 3-5, respectively.

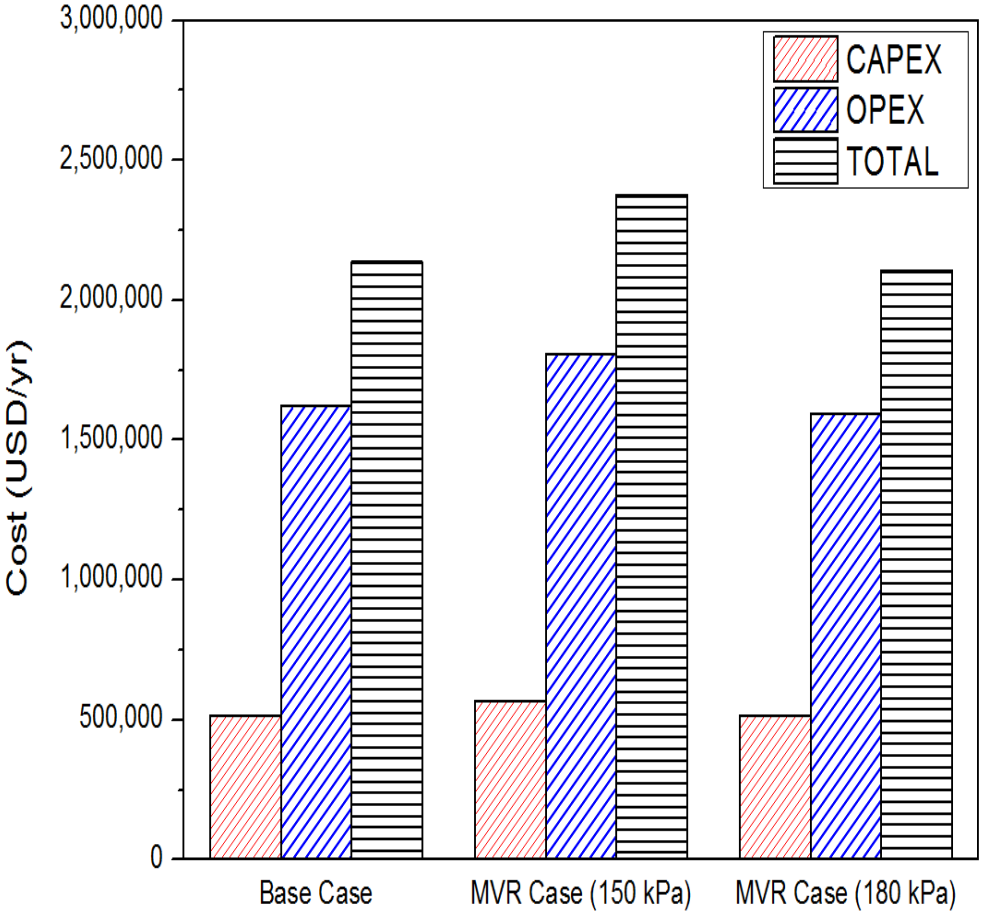

Fig. 3-5 Total annualized costs for each simulation scenario

Table 3-3. Summary of process equipment costs (from Aspen Process Economic Analyzer)

	Base Case	**MVR Case (1.5 bar)**	**MVR Case (1.8 bar)**
Type Of Equipment	Cost (US$)	Cost (US$)	Cost (US$)
CO_2 Absorber column	121,800	121,800	121,800
CO_2 Stripper column	89,800	64,300	64,300
HX and Pump for capture process	63,800	63,800	64,100
CO_2 Compressor unit	1,721,600	2,016,600	1,736,600
HX and Pump for comp. process	67,320	38,200	38,200
Total Equipment Cost	2,064,320	2,304,700	2,025,000

Table 3-4. Summary of capital cost investment (CAPEX)

			Base Case	MVR Case (1.5 bar)	MVR Case (1.8 bar)
	% of FCI	**Used**	**Cost (US$)**	**Cost (US$)**	**Cost (US$)**
Direct cost					
ISBL					
Purchased equipment	20-40%	30%	2,064,320	2,304,700	2,025,000
Purchased equipment installation	7.3-26%	10%	688,107	768,233	675,000
Instrumentation and control	2.5-7.0%	5%	344,053	384,117	337,500
Piping	3-15%	10%	688,107	768,233	675,000
Electrical	2.5-9.0%	5%	344,053	384,117	337,500
OSBL					
Building and building services	6-20%	8%	550,485	614,587	540,000
Yard improvements	1.5-5.0%	2%	137,621	153,647	135,000
Services facilities	8.0-35.0%	8%	550,485	614,587	540,000
Land	1-2%	2%	137,621	153,647	135,000
Total Direct Cost		80%	5,504,853	6,145,867	5,400,000
Indirect cost					
Engineering	4-21%	5%	344,053	384,117	337,500
Construction expenses	4.8-22.0%	5%	344,053	384,117	337,500
Contractor's fee	1.5-5.0%	5%	344,053	384,117	337,500
Contingency	5-20%	5%	344,053	384,117	337,500
Total Indirect Cost		20%	1,376,213	1,536,467	1,350,000
Fixed capital investment (FCI)	100%		6,881,067	7,682,333	6,750,000
Working Capital	10-20%	15%	1,032,160	1,032,160	1,152,350
Total Capital Investment (CAPEX)	NPV		**7,913,227**	**8,714,493**	**7,902,350**
Annualized capital costs (r=5%, t=30 years)	EAC		**514,767**	**566,890**	**514,059**

Table 3-5. Summary of operating cost expenditure (OPEX)

			Base Case	MVR Case (1.5 bar)	MVR Case (1.8 bar)
	Range	**Used**	**Cost (US$)**	**Cost (US$)**	**Cost (US$)**
Fixed Charge (FC)			220,194	245,835	216,000
Local Taxes	1-4%	3%	172,027	192,058	168,750
Insurance	0.4-1%	0.7%	48,167	53,776	47,250
Direct Production Cost (DPC)			757,478	844,849	743,480
Cooling Water (Seider 2004)	$0.013/cum		160	0	0
LP Steam (50 psig; Seider 2004)	$5.50/1000kg		5,157	4,102	4,194
Electricity (US DOE 2010)	$0.065/kWh		3,756	5,442	5,008
Maintenance (M)	1.0-10% FCI	5%	344,053	384,117	337,500
Operating Labor (OL)	10-20% Total Prod Cost	15%	243,272	271,428	238,726
Supervision and support labor (S)	30% of OL		72,981	81,428	71,618
Operating Supplies	10-20% M	15%	51,608	57,618	50,625
Laboratory charges	10-20% OL	15%	36,491	40,714	35,809
Plant Overhead Cost (OVHD)	50-70% of (M+OL+S)	60%	396,184	442,184	388,706
Total Manufacturing Cost	FC+DPC+OVHD		1,373,856	1,532,867	1,348,186
General Expenses					
Administrative Cost	15-20 % of OL	17.5%	42,573	47,500	41,777
Distribution and Marketing	2-20% OPEX	11%	155,807	173,840	152,896
R&D Cost	2-5% OPEX	3.5%	49,575	55,313	48,649
Total Product Cost (OPEX)			**1,621,811**	**1,809,520**	**1,591,508**

3.3. Results and discussion

In this chapter, post-combustion CO_2 capture process was modeled and validated against the actual operating data of existing plant in Boryeong, South Korea. A CO_2 compression process was also modeled using actual design data of existing test bed. Implementing MVR process for CO_2 capture is beneficial for not only capture process itself, but can also be economically beneficial for the compression process. In order to determine the optimal operating pressure for MVR process, thermodynamic analysis including energy and exergy efficiency as well as economic evaluation were performed. In terms of exergy efficiency, MVR process starting from 1.5 bar has less amount of exergy destroyed for stripper column. However, when economic evaluation is also considered, MVR process at 1.8 bar is a better option because it not only reduces the amount of exergy destroyed for stripper column, but also reduces the capital and operating costs for CO_2 capture and compression processes. In particular, reduction in compressor cost has a significant impact on the economic evaluation. At this condition, the amount of energy reduction, destroyed exergy reduction, and annualized costs reduction corresponds to 8.43%, 34.7%, and 1.5%, respectively. Thermodynamic analysis considering

energy and exergy is valuable for a deep understanding of processes. But for an economic optimization, total production cost considering CAPEX and OPEX have to be taken into account, being highly dependent on the actual site. Even though for this article, the price of electricity is overestimated in the U.S. standards, the price of electricity for industrial use is much lower in Korea, which means that it will have greater saving effects when implemented in Korean standards. Currently, the MVR process design is under consideration to be included for Korean Government's demonstration project of large-scale post-combustion capture plant before 2020. The saving effect of this process configuration will be further investigated during the actual design phase in the future.

CHAPTER 4. Modeling of the Pre-combustion CO_2 Capture Process

4.1. Process overview

Unlike post-combustion capture of CO_2, pre-combustion capture refers to removing CO_2 from fossil fuels before combustion takes place. For example, in gasification processes a feedstock (coal, biomass, etc.) is partially oxidized in steam and excess oxygen from air separation unit (ASU) at high temperature and pressure to produce synthesis gas, also known as syngas which consists of H_2, CO, CO_2, and smaller amounts of other gaseous components, such as CH_4. The syngas then goes through the water-gas shift (WGS) reaction to produce a H_2 and CO_2-rich gas mixture. The concentration of CO_2 in this mixture can range from 15-60%, then the CO_2 can be captured and compressed for transportation.[30-32] The most common example of pre-combustion is Integrated Gasification Combined Cycle (IGCC) shown in Fig. 4-1, which is known to have higher efficiency than the conventional coal power plants. Commercially available pre-combustion carbon capture technologies typically use physical or chemical absorbents which cost around $60/ton to capture CO_2 generated by an integrated gasification

combined cycle (IGCC) power plant. Although main research trend in this area rather focuses on separation technologies by developing advanced absorbents or membranes, in this thesis, process optimization based on modeling and simulation will be focused which will eventually lead to reduce the capture costs level of CO_2 near $40/ton. Main advantages and disadvantages of the pre-combustion capture is summarized in Table 4-1.

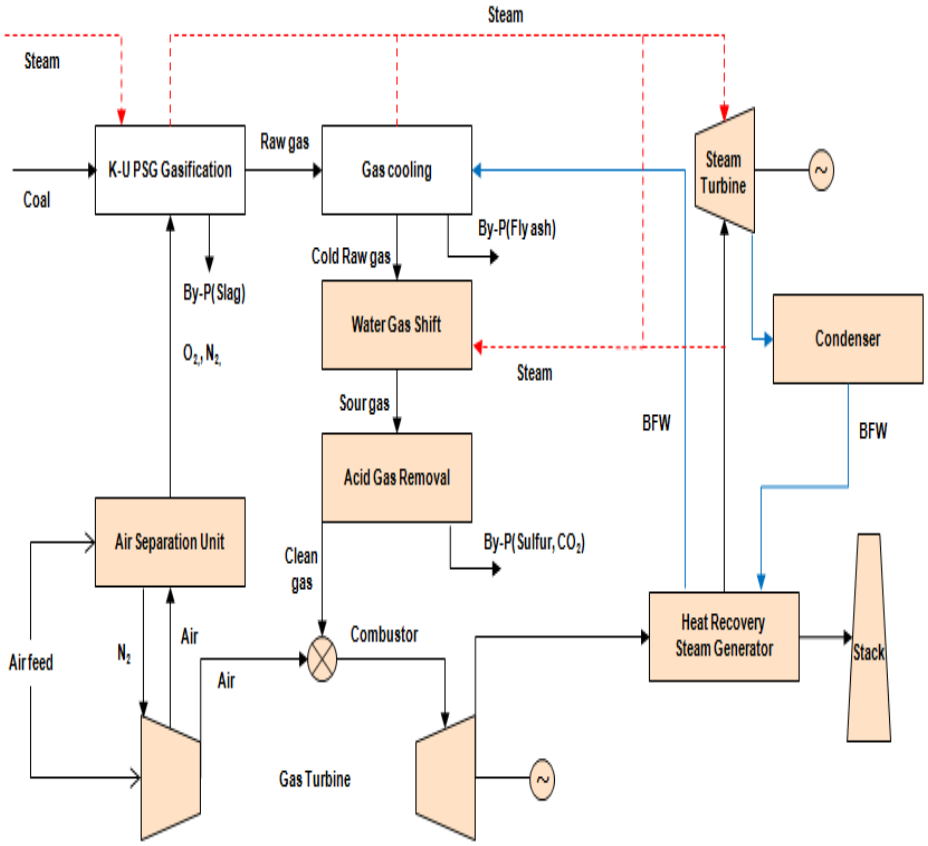

Fig. 4-1 Block flow diagram of the IGCC plant

Table 4-1. Advantages and disadvantages of pre-combustion capture

Advantages	Disadvantages
- Low energy consumption for absorbent regeneration - CO_2 at high pressure	- High capital investment - Applicability (no retrofit)

4.2. Process modeling and simulation

IGCC plant mainly consists of several unit processes: Gasifier, Air Separation Unit (ASU), Water-Gas Shift (WGS) reactor, Acid Gas Removal (AGR) unit, and Combined Cycle for electricity generation. Each unit process is modeled with Aspen Plus (V7.3) based on the data from literature or licensor companies. Licensor data from Air Liquide and UOP for selected unit processes were provided with courtesy of KEPRI (KEPCO Research Institute), and the source for modeling is shown in Table 4-5. Among above-mentioned unit processes, gasifier unit was simply modeled in a black-box format due to limited data availability and confidentiality.

Table 4-2. Data source for modeling unit processes

Unit process	Licensor	Commercial name/description
ASU	Air Liquide	Air Liquide Cryogenic
WGS	Haldor Topsoe	AS CO Shift
AGR	UOP	SeparALL™
CC	-	300MW IGCC Plant design data

4.2.1. Air separation unit (ASU)

Air separation unit (ASU) separates oxygen from air to provide excess air into the gasifier for partial oxidation.[33] Among many available technologies, cryogenic separation process was chosen because it is most widely used commercialized process since 1290s.[34, 35] The process flow diagram of cryogenic separation are shown in Fig. 4-2. Air is first compressed by main air compressor and dried in a purification unit, typically using molecular sieves. Treated air is cooled to the liquefaction temperature, and distilled into oxygen and nitrogen which are subsequently heated and vaporized, producing oxygen product with purity above 95% for the IGCC plant. ASU process has 2 distillation column: one at lower pressure (LPC at 1.37 bar) and the other at higher pressure. (HPC at 6.21 bar)

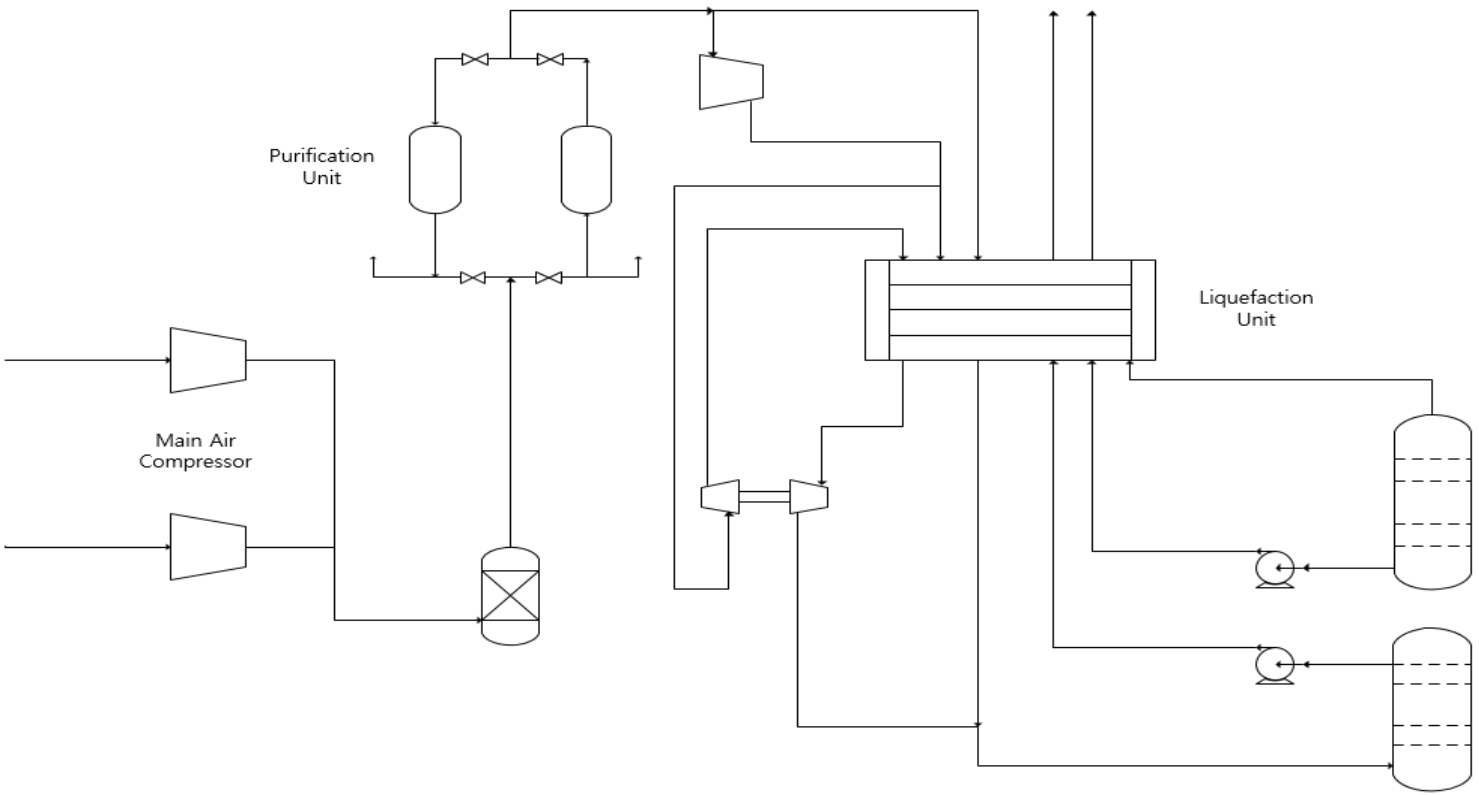

Fig. 4-2 Process flow diagram of cryogenic ASU

4.2.2. Water-gas shift reactor (WGS)

Water-gas shift (WGS) reactor includes chemical reactions which convert the syngas (H_2O, CO) into H_2 and CO_2-rich product. In the shift reactors, the CO in the syngas is converted to CO_2 by the water gas shift reaction written below, so that more CO_2 can be effectively captured in the acid gas removal process following the WGS. [36]

$$CO + H_2O \leftrightarrow H_2 + CO_2 \qquad \Delta H = \text{-41 kJ/mol}$$

Since this reaction is exothermic, the equilibrium constant decreases with increasing temperature which eventually leads to low CO conversion. Carbonyl sulfide is converted to hydrogen sulfide through hydrolysis via reaction written below.

$$COS + H_2O \leftrightarrow H_2S + CO_2 \qquad \Delta H = \text{-30 kJ/mol}$$

Choosing the appropriate reactor model is very important, but the type of reactor used for WGS reactor is limited since detailed kinetics are not considered for modeling purpose. 4 types of reactor models can be considered: RStoic, RYield, RGibbs, REquil. Simulation test was performed as shown in Fig. 3-3, and the results are shown in Table 3-2. According to the results, either RStoic or RYield models are the most suitable models for Aspen simulation, and RStoic model was used in this study.

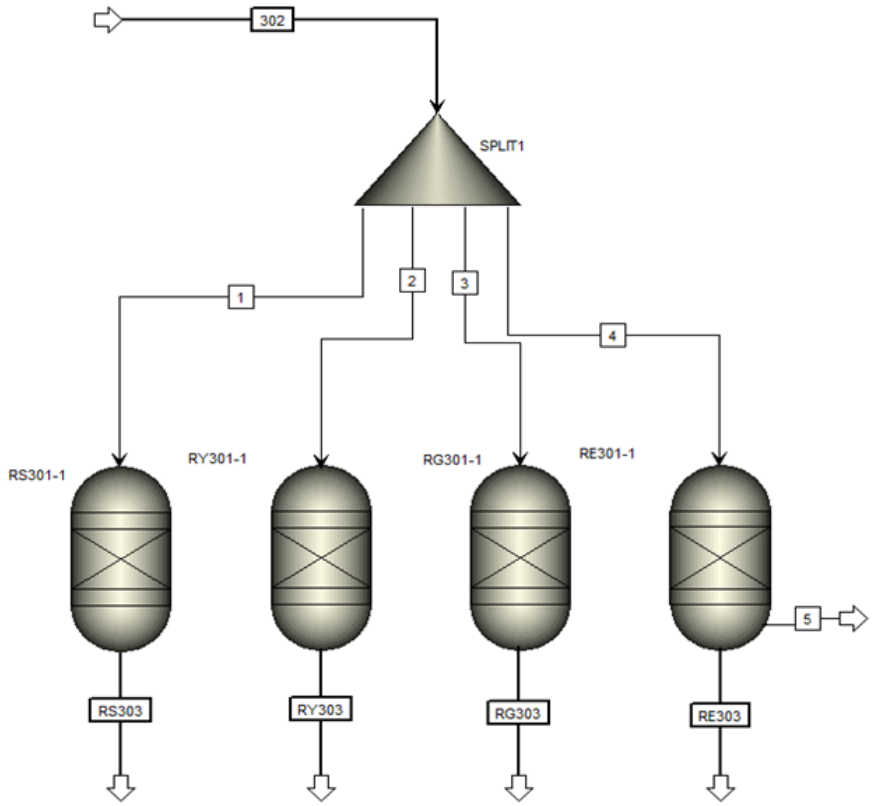

Fig. 4-3 Reactor modeling with different reactor types

Another important decision factor is thermodynamic model, and the most appropriate property method was chosen based on the tree structure shown in Fig. 3-4. Among 5 types of property methods, (PENG-ROB, RK-SOAVE, LK-PLOCK, PR-BM, RKS-BM) Peng-Robinson equation of state was selected because it is the most practical and flexible method for a variety of chemical processes. The process flow diagram for the WGS process is shown in Fig. 3-5.

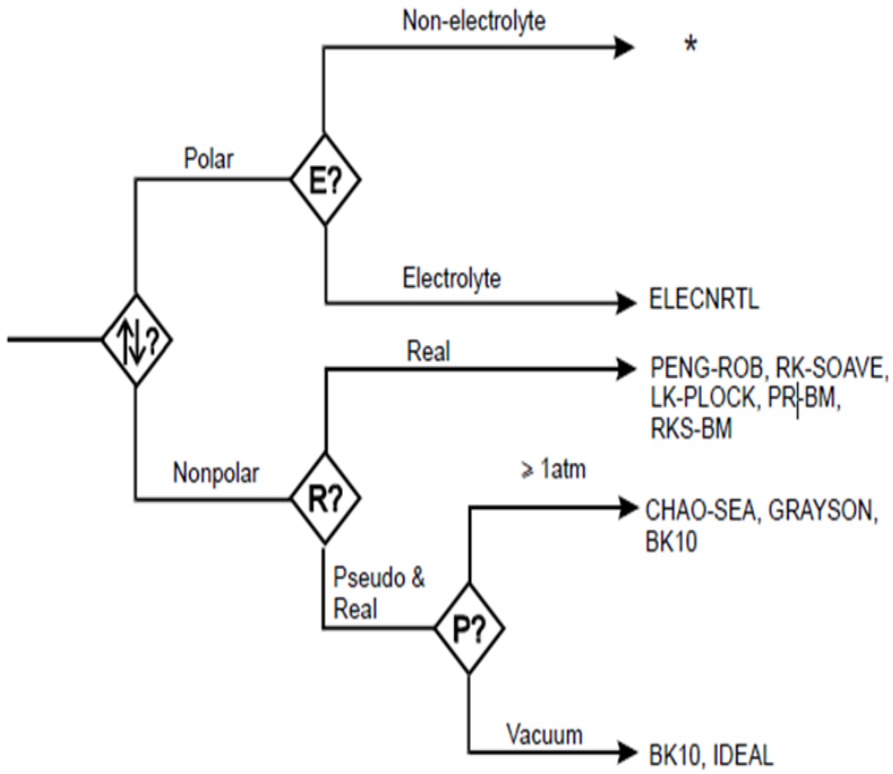

Fig. 4-4 Selection tree of Aspen property method (Equation of State)

Table 4-3. Simulation test results for different Aspen reactor models

	303	RS303		RY303		RG303		RE303	
Temperature C	470	470		470		470		470	
Pressure barg	36.1	36.1		36.1		36.1		36.1	
Mole Flow kmol/hr	25253	25321.377	-68.377	25325.275	-72.275	24483.37	769.63	25359.177	-106.177
Mass Flow kg/hr	486885	486885	0	486885	0	486885	0	486885	0
Mole Frac									
H2O	0.2636	0.263	0.0006	0.264	-0.0004	0.239	0.0246	0.256	0.0076
CO2	0.247	0.248	-0.001	0.247	0	0.306	-0.059	0.254	-0.007
H2S	0.0004	0	0.0004	0	0.0004	0	0.0004	0	0.0004
COS	0.0000066	0	0.0000066	0	0.0000066	0	0.0000066	0	0.0000066
H2	0.3883	0.389	-0.0007	0.388	0.0003	0.401	-0.0127	0.397	-0.0087
CO	0.0686	0.068	0.0006	0.069	-0.0004	0.003	0.0656	0.062	0.0066
N2	0.0311	0.031	1E-04	0.031	1E-04	0.032	-0.0009	0.031	1E-04
AR	0	0	0	0	0	0	0	0	0
CH4	0.0008	0.001	-0.0002	0.001	-0.0002	0.018	-0.0172	0	0.0008
NH3	0.0003	0	0.0003	0	0.0003	0	0.0003	0	0.0003
HCN	0	0	0	0	0	0	0	0	0

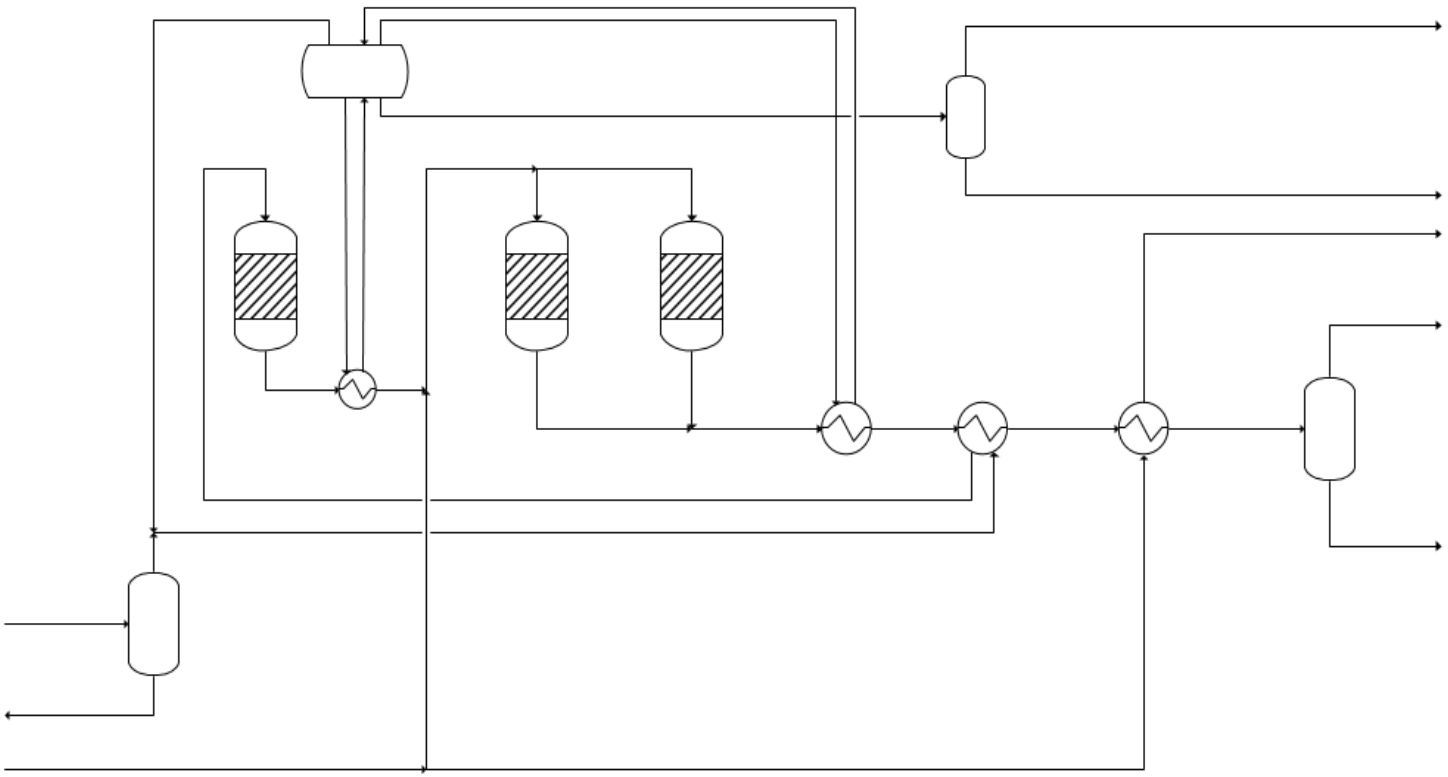

Fig. 4-5 Process flow diagram of WGS unit

4.2.3. Acid gas removal unit (AGR)

Acid gas removal (AGR) unit in the IGCC plant is the process which distinguishes IGCC from the post-combustion capture. This process basically consists H_2S and CO_2 removal section, which can be differentiated based on the type of solvent used for acid gas removal. 3 major types of solvents are: chemical, physical, and hybrid solvents.[37] Some of the most common chemical and physical solvents are tabulated in Tables 3-3 and 3-4, respectively.

Table 4-4. Examples of common chemical solvents

Solvent	Name	Main licensors
Monoethanolamine	MEA	Dow, UOP, Fluor
Diethanolamine	DEA	Elf, Lurgi
Diglycolamine	DGA	Texaco, Fluor
Methyldiethanolamine	MDEA	BASF, Dow, Shell
Hindered amine	AMP etc.	Exxon
Potassium Carbonate	HotPot etc.	Union Carbide, Eickmeyer

Table 4-5. Examples of common physical solvents

Solvent	Name	Main licensors
Dimethyl ether or poly-ethylene glycol (DEPG)	Selexol	UOP
Methanol	Rectisol	Linde, Lurgi
N-methyl pyrrolidone	Purisol	Lurgi
Polyethylene glycol and dialkyl ethers	Sepasolv	BASF
Tetrahydrothiophenedioxide	Sulfolane	Shell

The type of solvent used for acid gas removal can be determined by many different criteria such as treated gas specification or selectivity between H_2S and CO_2, for example. Operating condition, especially pressure, is an important criterion to determine which solvent can be used for a given AGR unit. In the IGCC case, AGR process is operated at a relatively high pressure about 50 bar. As shown in Fig. 4-6, physical solvent has better loading capacity than chemical solvent at high pressure range. Besides, as mentioned before, physical solvent consumes a relatively less amount of energy for solvent regeneration than chemical solvents do. Profess flow diagram for AGR unit is shown in Fig. 4-7, which includes H_2S absorber, CO_2 absorber, and solvent regenerator. Selexol solvent is used to remove the acid gas and PC-SAFT property method is used for process simulation. [39]

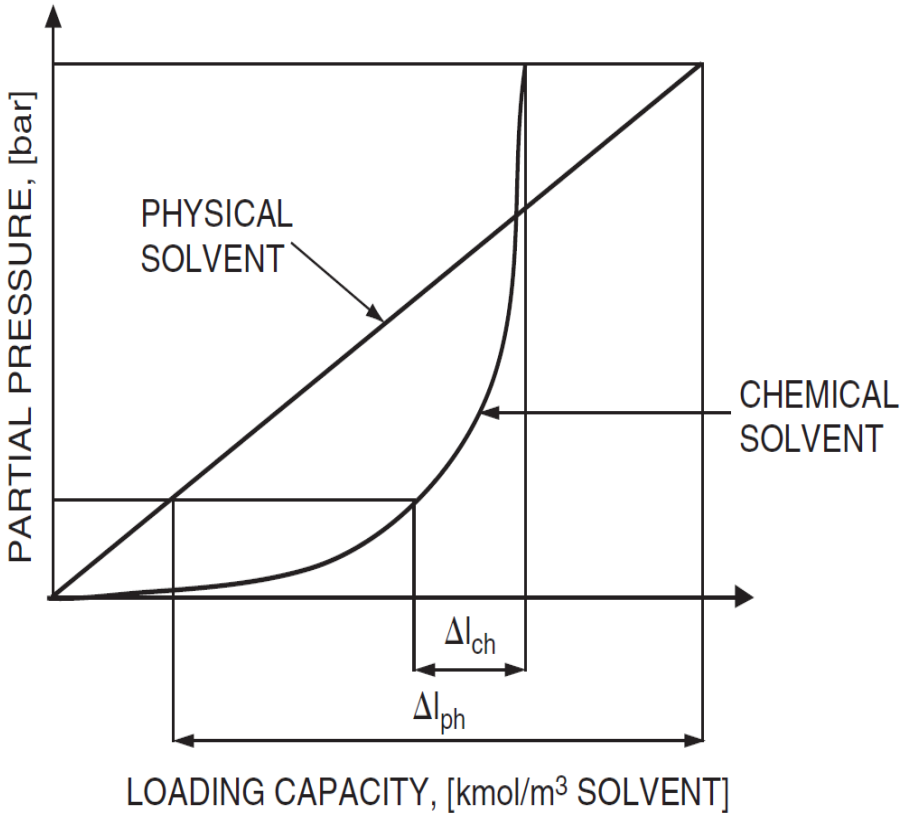

Fig. 4-6 Comparison of loading capacity between solvents [38]

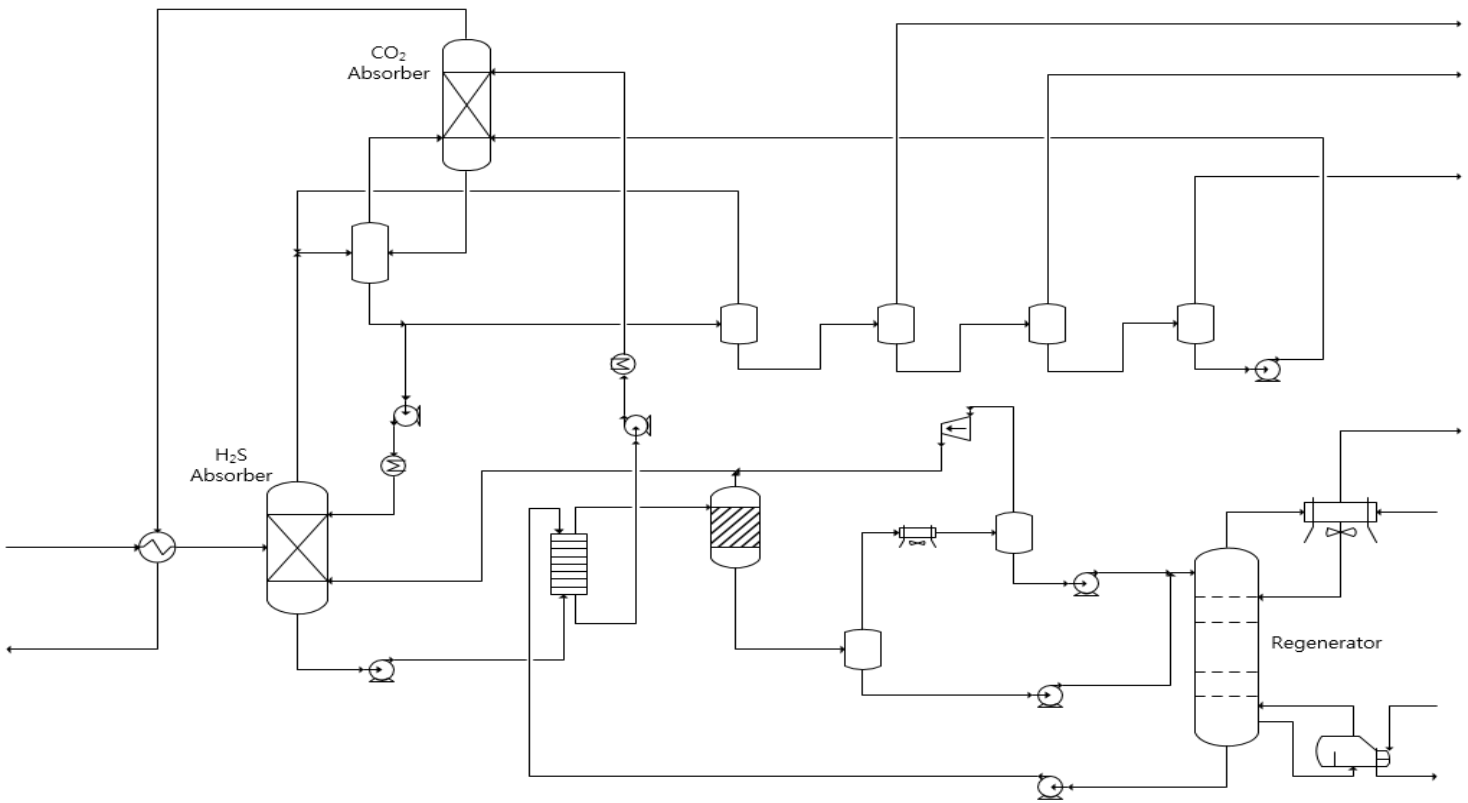

Fig. 4-7 Process flow diagram of the AGR unit

4.2.4. Combined Cycle system (CC)

IGCC plant implements a combined cycle system which consists of Gas Turbine (G/T), Steam Turbine (S/T) and Heat Recovery Steam Generator (HRSG). It is responsible for electricity generation where Brayton and Rankine cycles are integrated to achieve higher power output. Basic configuration for the combined cycle is taken from the preliminary design data of 300MW IGCC plant in Taean, South Korea. Since process configuration for the combined cycle could not be fully disclosed due to confidential issues, a common example and simplified flow diagrams of combined cycle steam are shown in Figures 4-8 through 4-10.

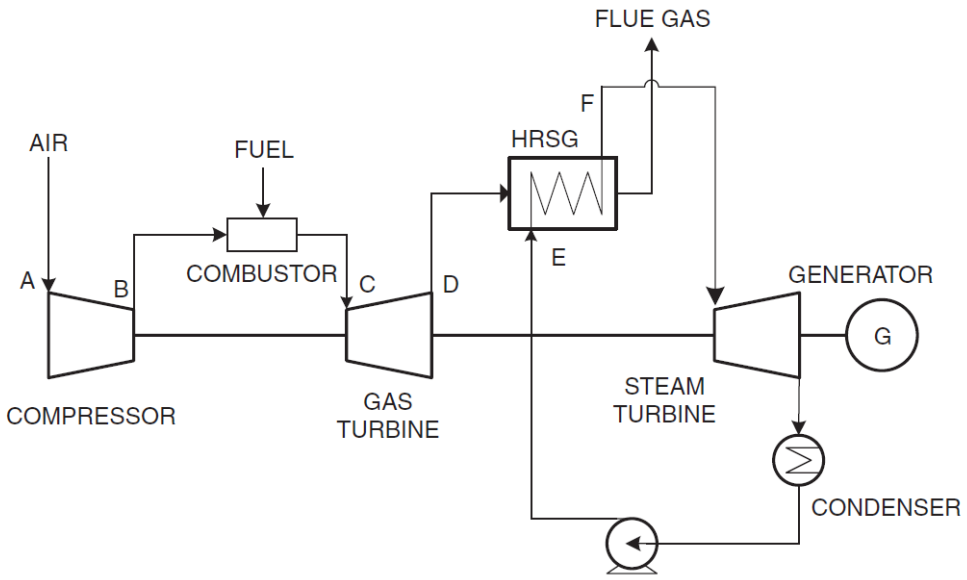

Fig. 4-8 Common process configuration for the combined cycle [38]

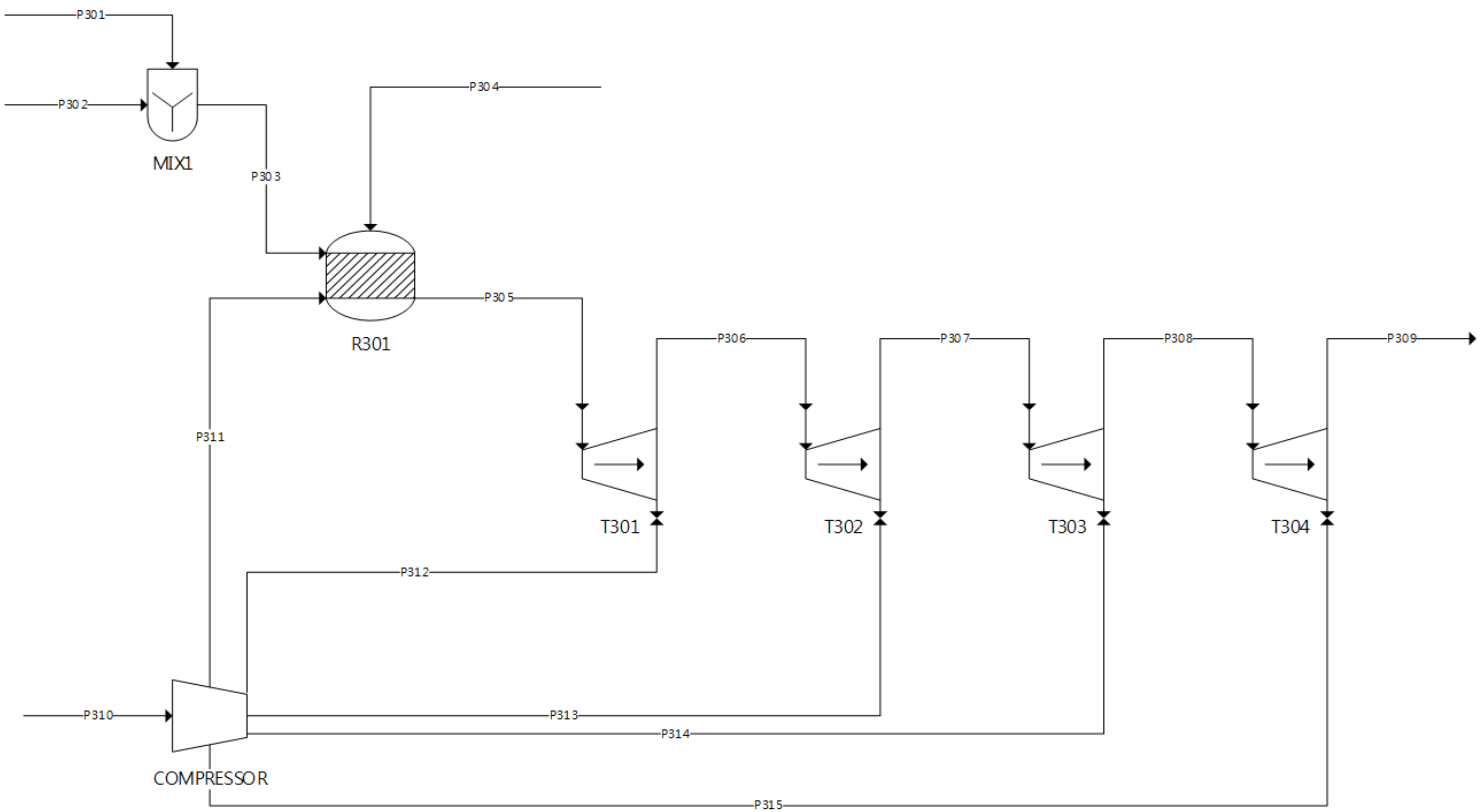

Fig. 4-9 Simplified process flow diagram for gas turbine

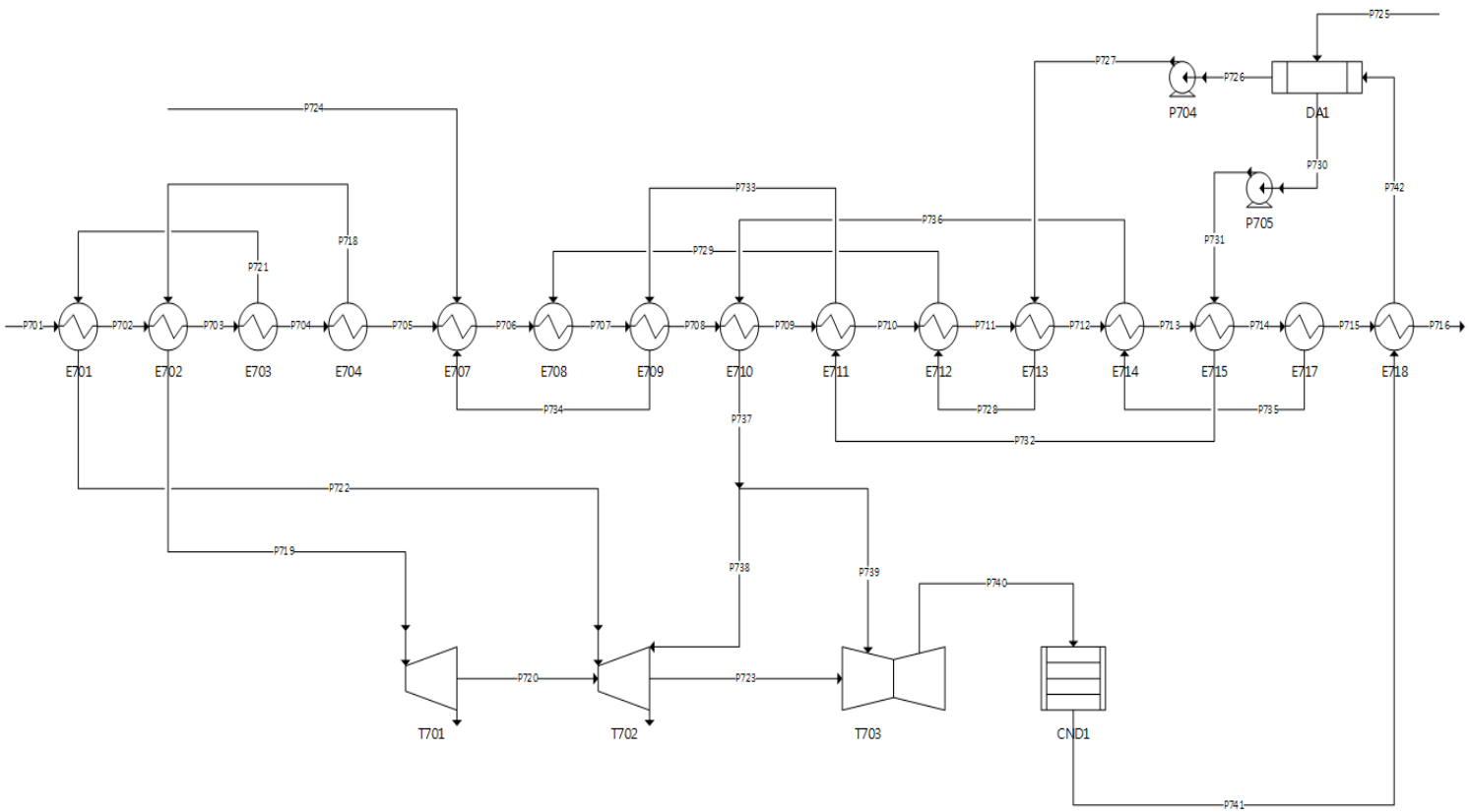

Fig. 4-10 Simplified process flow diagram for steam turbine and HRSG

The gas turbine system used in the actual IGCC plant is modified from commercial gas turbines originally designed for natural gas use, so technical issues such as compressor surge control, turbine rotor torque, inlet temperature or blade durability must be considered in the actual operation. However, these factors could not be taken into account in the modeling phase, so Ideal property method was chosen for the thermodynamic model. Also for the combustor, RStoic model in Aspen Plus was used which can simulate the combustion reaction. For the compressor model, polytropic using ASME method type was used with assumed efficiency of 90%. For the turbine model, isentropic type was used for all 4 turbines each with efficiency of 86.57, 86.56, 86.56, and 80.04%, respectively.

For the steam turbine system and HRSG, it has more complicated structure than the gas turbine case because additional equipments are required for heat recovery purpose. HRSG system includes 3 different pressure levels, each level with reheater, superheater, evaporator, and economizer. Since steam turbine and HRSG process only uses water and steam, STEAMNBS property method was used for the thermodynamic model, which can simulate the water-steam system between 273.15 and 2,000 K. [40]

4.3. Results and discussion

The overall block flow diagram for the IGCC plant model is shown in Fig. 4-11, where all of unit processes are interconnected in hierarchy blocks in Aspen Plus. Since all of the input data were directly taken from the reference or licensor data, further validation was not performed. However, it was possible to compare the performance of the turbines based on the values shown in Tables 4-5 and 4-6, which show a reasonable agreement between plant design data and Aspen simulation results.

Table 4-6. Comparison of gas turbine performance

	Design data	**Simulation**	**Error**
Gas Turbine output (MW)	364	374	2.7%
Exhaust gas temperature (^{o}C)	601	599	0.3%
Exhaust gas flowrate (kg/hr)	2,655,522	2,655,524	0.0%

Table 4-7. Comparison of steam turbine performance

	Design data	**Simulation**	**Error**
Steam Turbine output (MW)	196	192	2.0%
Flue gas temperature (^{o}C)	101	109	7.0%
Flue gas flowrate (kg/hr)	2,655,523	2,655,523	0.0%
Steam flow to G/T (kg/hr)	17,529	17,529	0.0%

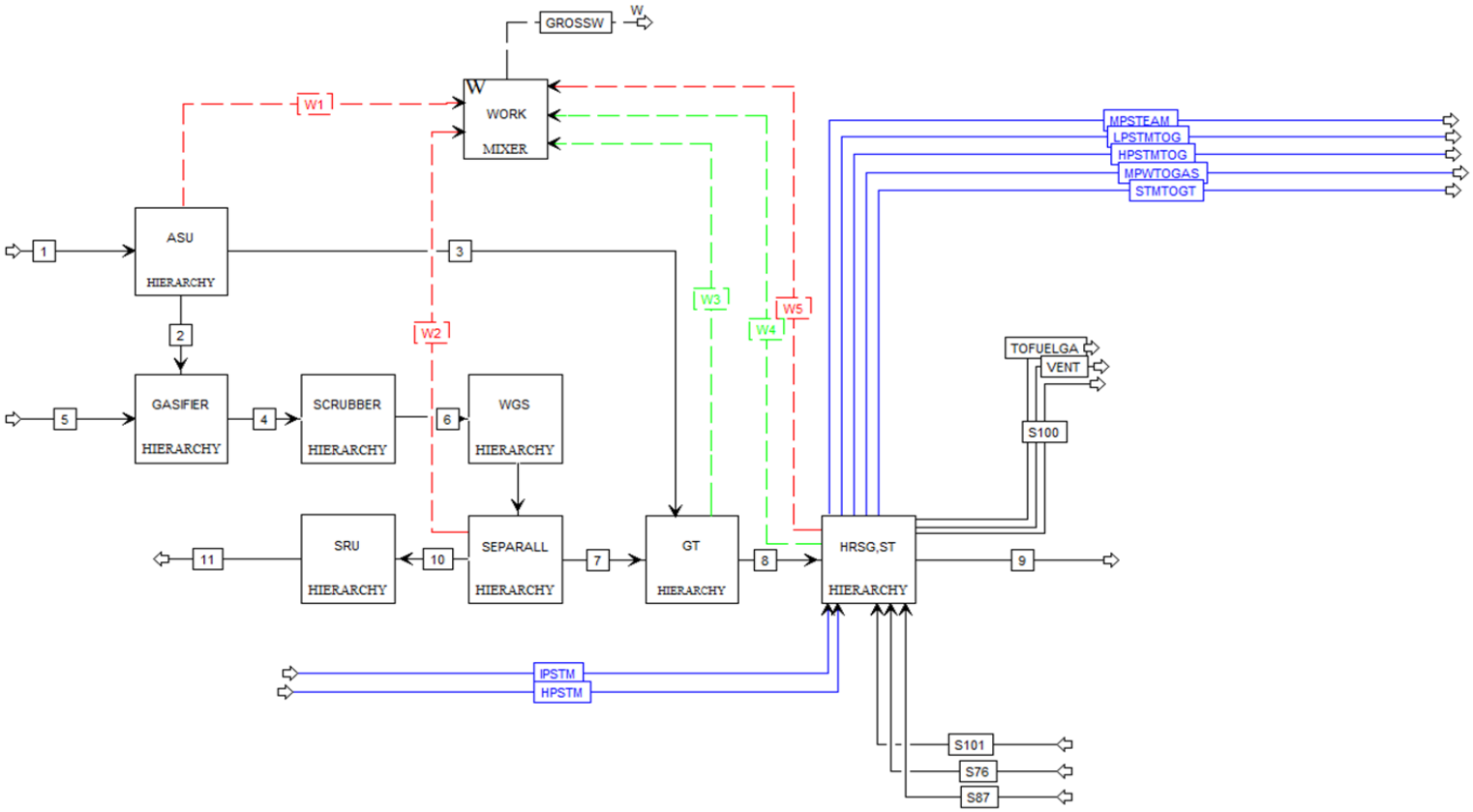

Fig. 4-11 Aspen flowsheet of the IGCC plant model

CHAPTER 5. Analysis of the Pre-combustion CO_2 Capture Process

5.1. Overview

In this chapter, pre-combustion CO_2 capture process is modified in order to reduce energy consumption to enhance process efficiency. Because the solvent regeneration step in the CO_2 capture processes consume a significant amount of energy, the process modification is essentially focused on retrofit of stripper configuration. Two vapor recompression processes are introduced to the stripper configuration: mechanical vapor recompression (MVR) for post-combustion capture and lean vapor compression (LVC) for pre-combustion capture, respectively. Especially for the pre-combustion capture, substitute natural gas (SNG) production process is investigated, which has a very similar process configuration as that of the IGCC plant. SNG is a methane-rich replacement for natural gas, and it can provide an excellent opportunity to address energy as well as environmental challenges in an economical and practical way.

5.2. Lean vapor compression (LVC) for AGR unit

Process design of the pre-combustion capture process is not as flexible as in the post-combustion capture, and plant retrofit is very limited for the IGCC plant. Although research on mechanical aspects such as turbines or heat exchangers exists which aims to enhance the plant efficiency, not much research has been done for the process alternatives or configuration modifications. In this section, a concept of lean vapor compression (LVC), which has been adopted from the post-combustion scenario, is implemented in acid gas removal (AGR) unit of the IGCC plant. [41-44] As can be seen in Fig. 5-1, a conventional AGR unit is essentially same as the post-combustion capture process because it can capture CO_2 using chemical or physical solvents and the solvents in the column need to be regenerated using thermal energy.

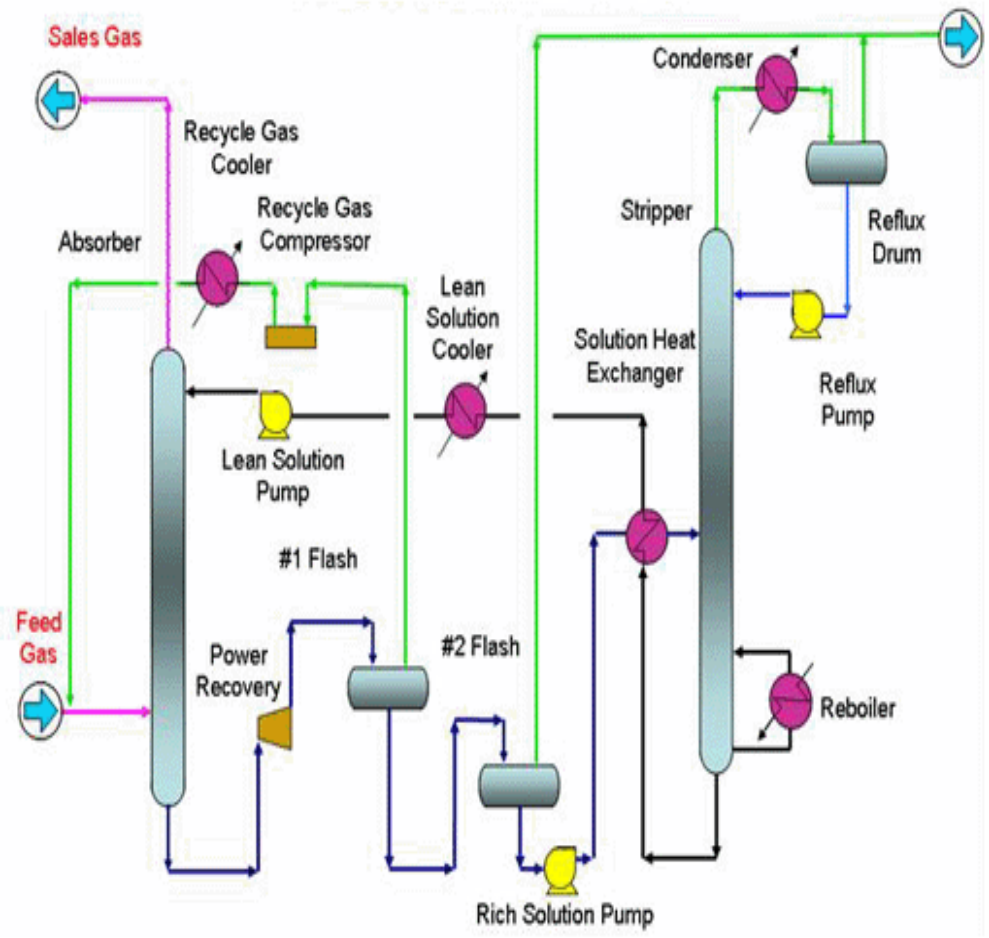

Fig. 5-1 Process schematics of AGR unit using BASF's OASE solvent

5.2.1. Process description

Fig. 5-2 shows the process flow diagram of LVC process. This process requires an expansion valve, a flash vapor/liquid separator and a steam compressor to the conventional CO_2 stripper column. The lean amine stream regenerated from the reboiler is expanded by V-1 valve and then sent to flash separator (D-1). Flashed vapor stream must be compressed (C-1) up to the stripper bottom pressure before re-entering the column. Because of the isentropic expansion in the V-1, the liquid lean amine temperature decreases in comparison with the base case. As a result, heat exchanger duty of E-1 as well as the temperature of rich amine stream entering the stripper temperature also decrease.

LVC reduces thermal energy consumption in the stripper reboiler in two ways: First, recompressed steam re-entering the stripper bottom reduces the amount of steam required for the reboiler. Second, lowered inlet temperature for stripper feed stream reduces the latent heat requirement by decreasing the stripper top temperature. The energy saving effect of LVC has been proven in several projects worldwide, including the 10MW pilot plant in Boryeong Power Plant. However, additional costs for compressor and electricity costs must be taken into account to assess the actual saving effect.

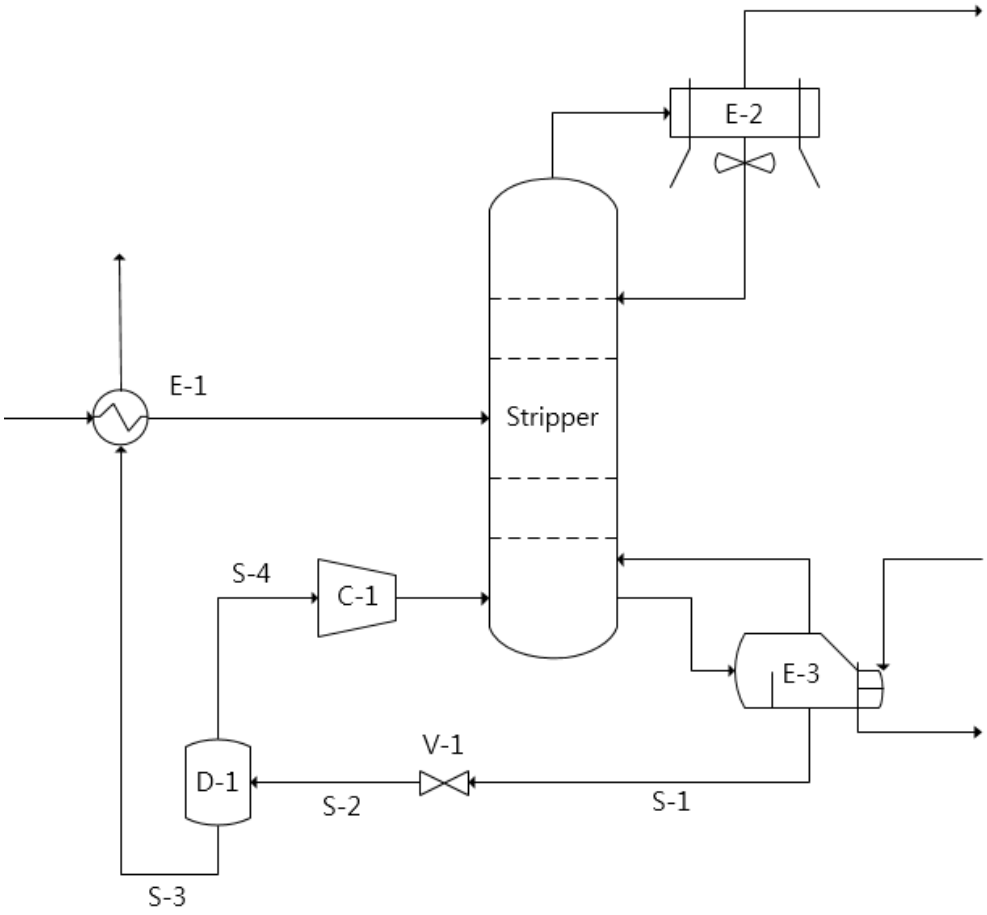

Fig. 5-2 Process schematics of the CO_2 stripper lean vapor recompression

5.2.2. Simulation results and analysis

The main design variables of LVC process are stripper pressure, expansion valve pressure, and minimum temperature approach of lean/rich amine heat exchanger. It is favorable to have a greater temperature difference between stripper operating pressure and the expansion pressure so that more steam can be generated. The energy balance for the loop created by LVC can be expressed in the equation below.

$$m_{S-1,original}\, C_p \Delta T_{S-1} = m_{S-3} C_p \Delta T_{S-3} + m_{S-4} \Delta H_{Vap} \qquad (5\text{-}1)$$

In the equation written above, $m_{S-1,original}$, m_{S-3}, and m_{S-4} indicate mass flow rate of stream S-1 of the base case, S-3, and S-4 of the LVC process, respectively. C_p and ΔH_{Vap} each represents the heat capacity and heat of vaporization of the stream. As mentioned in previous section, the temperature of lean amine stream (S-3) decreases compared to the base case without the LVC, which leads to a sensible heat recovery loss from the lean amine. However, this reduction is compensated by additional latent heat recovered by steam from the flash drum. [45]

Simulation results of the LVC process is shown in Table 5-1 below, with assumption that the most amount of steam is recovered using maximum pressure difference. Of course in this case, additional compression energy must be taken into consideration, and the same efficiency factor used in Chapter 3 (44.64%) was applied.

Table 5-1 Simulation results of LVC process in AGR unit

	Without LVC	With LVC
Reboiler heat duty (MW)	36.1	18.0
Lean/rich heat exchanger duty (MW)	49.9	33.7
Compressor duty (MW)	-	1.9
Regeneration energy (GJ/ ton CO_2)	0.38	0.23

Due to the nature of physical solvents, whose regeneration can be achieved not only with less thermal load but also with pressure swing, the regeneration energy significantly decreases compared to the chemical absorbents in post-combustion scenario. However, the price of physical solvents for CO_2 capture is known to be much higher.

5.3. Substitute Natural Gas (SNG) Production

Gasification technology is emerging as a possible solution to resolve the problems that coal had as a fuel source. Coal is not as efficient as other petroleum fuel, and also generates greenhouse gases after combustion. Besides, about 47% of world reserves of coal are low rank coal, which is difficult to be used in conventional pulverized coal power plant. [46] Natural gas is considered a cleaner type of fossil fuel, but its reserves are quite limited in comparison with coal. Natural gas production in general has been increasing due to advanced technologies, countries such as Korea or Japan still heavily depends on importing Liquefied Natural Gas (LNG) from overseas. In order to overcome the obstacles associated with high costs incurred by pipeline supplies or energy dependency, production of Substitute Natural Gas (SNG) is considered. SNG process is a conversion process to use coal more efficiently by chemical conversion from coal to methane, which is a primary component in natural gas. SNG process is also known as a clean technology with low emission of acid gas and has a high efficiency than other conversion processes. SNG projects are currently ongoing or planned in many countries over the world including the U.S., China, Korea, and India.

5.3.1. Process description

SNG production plant has a similar configuration to the IGCC plant, except for the methanation process which converts syngas to methane-rich SNG product. A block diagram of a conventional SNG plant using Thyssenkrupp's commercial gasifier technology is shown in Fig. 5-3, where major units are marked in colored boxes.

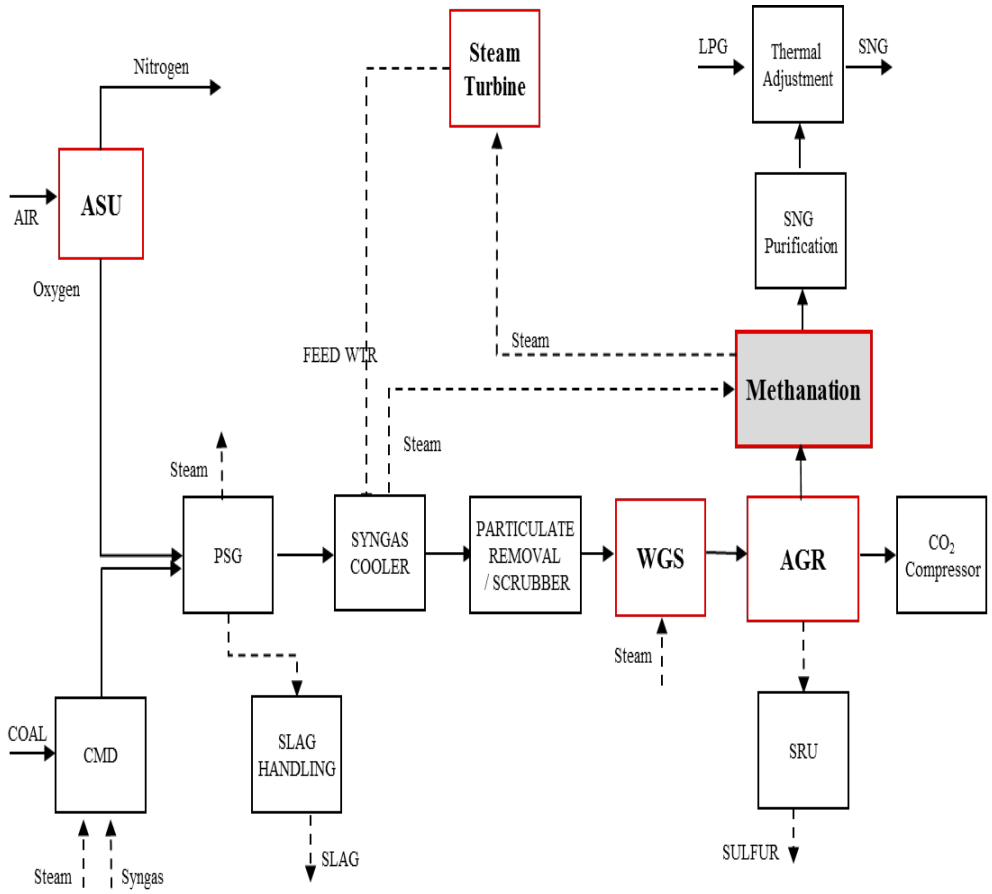

Fig. 5-3 Block flow diagram of the overall SNG production plant

Methanation reaction has been widely used as the final purification step in hydrogen and ammonia plants. It includes multiple reverse, exothermic reactions which hydrogenate both CO and CO_2. The composition of the raw gas entering the methanation process may change depending on the gasification technology as well as the acid gas removal requirements. [47, 48] Two types of chemical reactions are dominant: CO Methanation reaction (Eqs. (5-2) and (5-3)) which converts carbon oxides to methane, and the CO Shift reaction in Eq. (5-4). Since these reactions are exothermic, low temperature is favorable. [49]

$$\mathrm{CO} + 3H_2 \leftrightarrow CH_4 + H_2O \quad (5\text{-}2)$$

$$\mathrm{CO_2} + 4H_2 \leftrightarrow CH_4 + 2H_2O \quad (5\text{-}3)$$

$$\mathrm{CO} + H_2O \leftrightarrow H_2 + CO_2 \quad (5\text{-}4)$$

Although it may depend on the properties of catalysts used, CO is much more reactive than CO_2.

5.3.2. Simulation and model validation

Methanation process was modeled with Aspen Plus (V7.3) using RSKMHV2 equation of state, and the simulation input data were taken from the literature whose model is based on the TREMP developed by Haldor Topsøe. [50] This process is widely implemented in several SNG projects worldwide including POSCO's 500,000 tons per year facility in South Korea. This model consists of three adiabatic reactors with intermediate cooling, and reactor model minimizes the Gibbs free energy of reaction which also takes into account the chemical equilibrium. [51] Although some of previous studies includes a steam turbine cycle as part of methanation process to generate electricity, steam turbine part was not considered for analysis in this study.

As shown in Fig. 5-4, multiple recycle structures are possible with three reactors. To eliminate some of the infeasible structures, MATLAB optimization function, fmincon, was coded to solve the objective function written below, which quickly solves constrained minimization problems. The relationship between Aspen Plus and MATLAB interfaces is shown in Fig. 5-5.

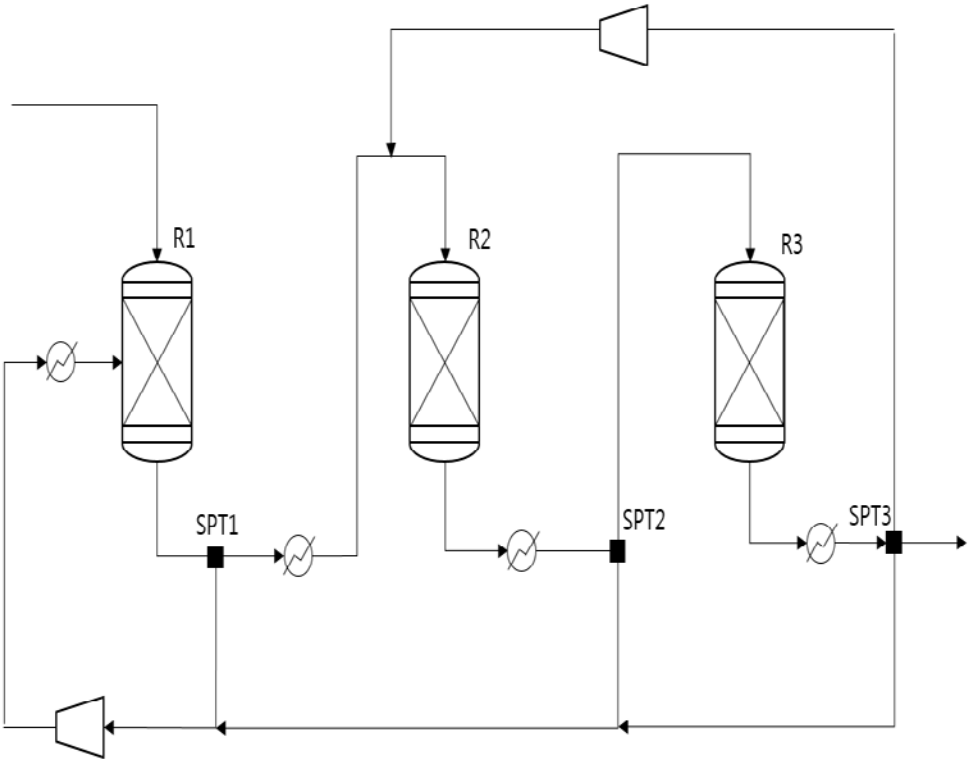

Fig. 5-4 Process diagram of the initial methanation process

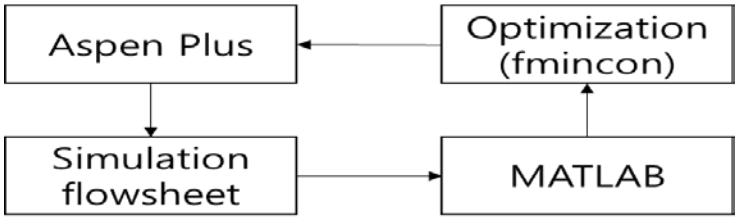

Fig. 5-5 Simulation-optimization linkage between Aspen Plus and MATLAB

Minimize $W_{comp}(SPT1, SPT2, SPT3)$

Subject to $0 < SPT1, SPT2, SPT3 < 1$;

$\mathrm{T}(R1_{out}) \leq 700℃$;

Mole fraction of $CH_4(R3_{out}) \geq 0.95$

Although it depends on the type of catalyst used for reactions, the temperature of high-temperature methanation reactor should not exceed 700℃ in order to avoid catalyst deactivation.[50] Also, the methane contents in the final SNG product must be greater than 95 mol%, which is a reference value used in a previous study.[52] According to the simulation results, it is more advantageous not to have any recycle from the second and third reactors, which significantly increase the amount of compressor duty. The base model used for model validation as well as technical and economic analysis is shown in Fig. 5-6, which has only one recycle structure after the first reactor. The intermediate cooling temperature between reactors is assumed to be 300℃, and pressure drops of 0.5 bar for reactors, 0.1 bar for coolers were assumed.

Validation of the base model was performed by comparing the simulation results with available data in the literature. [53, 54] Validation results are shown in Tables 5-1 and 5-2, respectively. The results indicate that this base model can simulate the methanation process precisely.

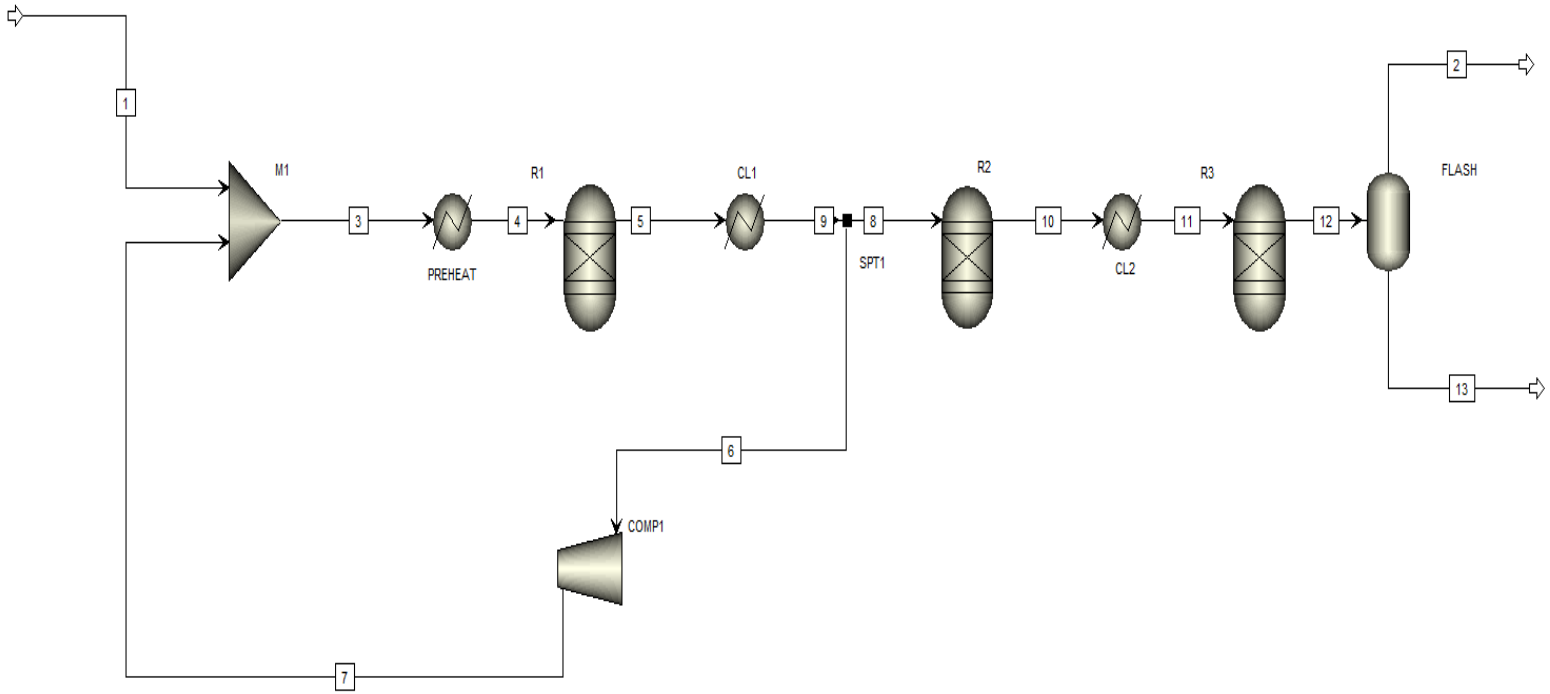

Fig. 5-6 Aspen Plus flowsheet of the base methanation model

Table 5-2. Model validation result of major units

	Unit	Li *et al.*	This work
Reactor			
R1 outlet temperature	℃	700	701
R2 outlet temperature	℃	523	522
R3 outlet temperature	℃	219	215
Compressor			
Outlet temperature	℃	304	304.6
Compressor duty	kW	617	735

Table 5-3. Model validation result of SNG product

		Unit	Li *et al.*	DOE	This work
SNG flow rate		kmol/hr	2033.1	-	2013.8
SNG composition					
	CH_4	mol %	94.6	94.95	96.1
	H_2		1.2	0.9	0.5
	CO_2		0.2	0.2	0.5
	N_2		2.8	2.8	2.7
	Ar		1.2	1.2	0.0
	CO		0.04	0.0	0.0

5.3.3. Technical analysis

Similar to the MVR scenario, exergy analysis was performed to determine the optimal operating conditions of the methanation process by varying the recycle ratio after the first reactor and the temperature of the intermediate coolers. Essentially, the amount of destroyed exergy, also known as the irreversibility of the process, can be determined using enthalpy and entropy values of a stream as written in Eqs. (3-1) and (3-2), which are easily calculated with simulator. [55] However, units which consume thermal or electrical energy require an additional correction term to calculate the exergy more appropriately, as written in Eqs. (5-5) and (5-6). [56]

$$\sum \dot{E}_Q = Q_{cooler}\left(1 - \frac{T_o}{T_{cooler}}\right) \quad (5\text{-}5)$$

$$\sum \dot{E}_W = T_0(s_i - s_0)_{comp} \quad (5\text{-}6)$$

$$T_0 = 298K$$

According to the literature, the biggest exergy destruction occurs in the first methanation reactor and heat recovery step following the first reactor [53]. To determine the amount of destroyed exergy, the recycle ratio after the first methanation reactor was varied, which is considered the most important parameter affecting the process performance. The breakdown of exergy destroyed for the base model is shown in Fig. 5-7. It can be concluded that the methanation process can have better operating conditions which reduce the

amount of destroyed exergy in the base model, especially from the first methanation reactor, which shows a good agreement with the previous study by Li *et al*.

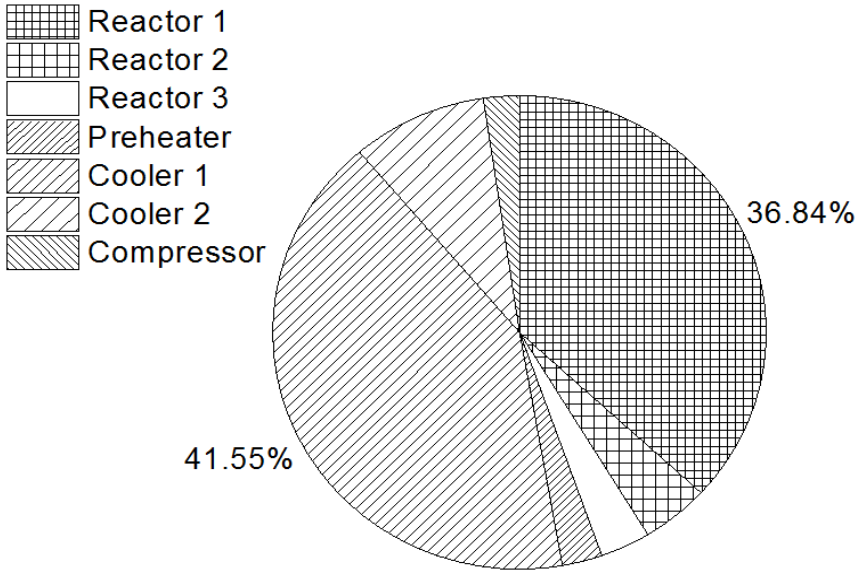

Fig. 5-7 Exergy destroyed for each unit operation in the base model

The amount of exergy destroyed with respect to the change in recycle ratio is shown in Fig. 5.8. Increasing the recycle ratio reduces the amount of exergy destroyed because it theoretically leads to higher efficiency in the first methanation reactor. As can be seen in Fig. 5.9, increasing the recycle ratio also reduces the outlet temperature of the first reactor, which is generally favorable for exothermic reaction. However, at high recycle ratio regime, the compressor duty requirement shows a sharp

increase, leading to a significant increase in electrical energy consumption. Although with increasing recycle ratio, both SNG flow rate and the methane composition slightly decrease as shown in Table 3. However, the extent is substantial compared to the exergy saving effects, which means that higher recycle ratio is still favorable.

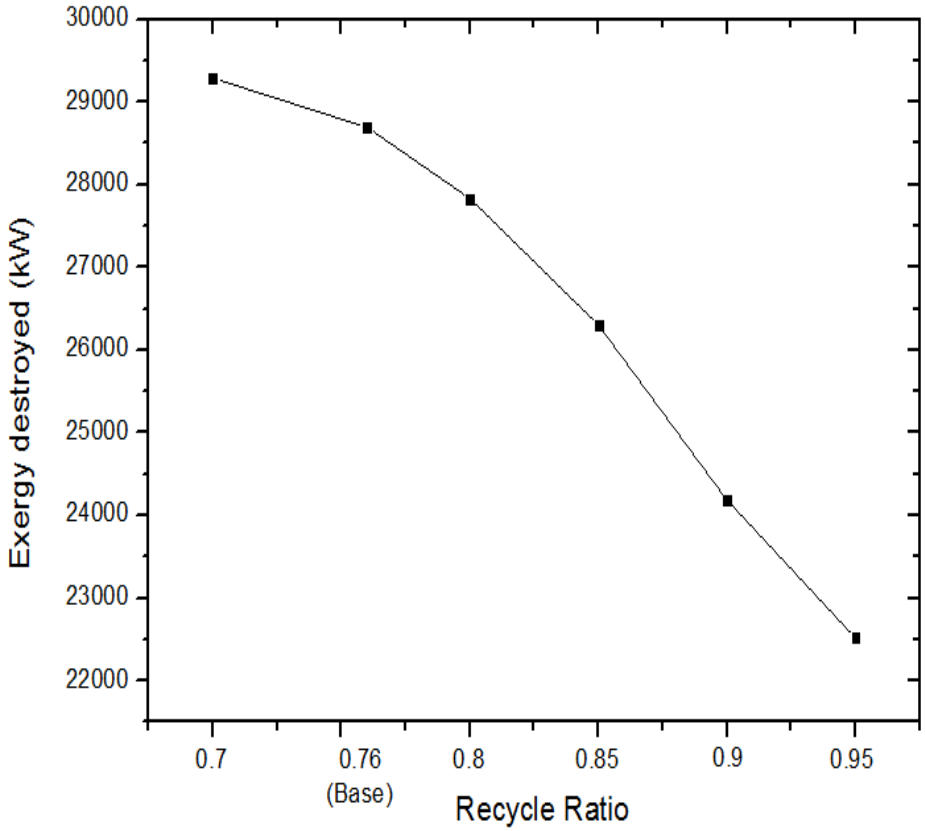

Fig. 5-8 Amount of exergy destroyed with change in recycle ratio

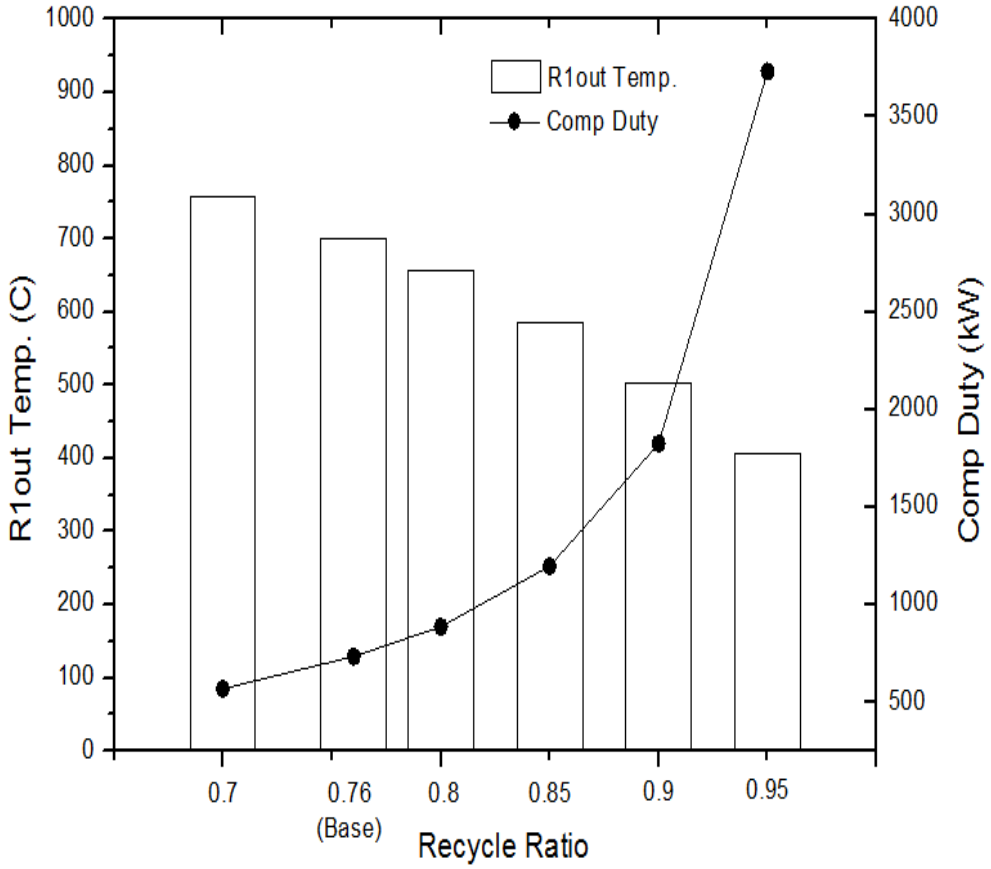

Fig. 5-9 Outlet temperature of the first reactor and required compressor duty

Table 5-4. Simulation results with different recycle ratio

Recycle ratio	**0.7**	**0.76 (Base)**	**0.8**	**0.85**	**0.9**	**0.95**
SNG production (kg/hr)	33,393	33,153	33,092	33,085	33,078	33,079
CH_4 composition (mol %)	94.5	96.1	96.6	96.7	96.7	96.7
R1 outlet temperature (℃)	758	701	656	587	503	407

Similarly, the intermediate temperature between the reactors was varied to observe the behavior of the exergy destroyed. Three intermediate cooling temperatures were considered at a fixed recycle ratio of 0.76, which is used in the validated model: 300℃ (base), 350℃, and 250℃. The results are shown in Table 5-4 and Fig. 5-10, respectively. The amount of destroyed exergy is reduced with increasing intermediate temperature. There also exists a trade-off relationship between the amount of destroyed exergy and the compressor duty. However, in 350℃ case, both reactor 1 outlet temperature and methane composition in the SNG product are not met, which makes the temperature infeasible at recycle ratio of 0.76. Based on the exergy analysis, it can be concluded that higher recycle ratio and intermediate temperature are favorable for the methanation process as long as the operation constraints are satisfied.

Table 5-5. Simulation results for different intermediate temperatures

Intermediate temperature	**250**℃	**300**℃ **(Base)**	**350**℃
SNG production (kg/hr)	33,089	33,153	33,408
CH_4 composition (mol %)	96.6	96.2	94.4
R1 outlet temperature (℃)	670	701	731

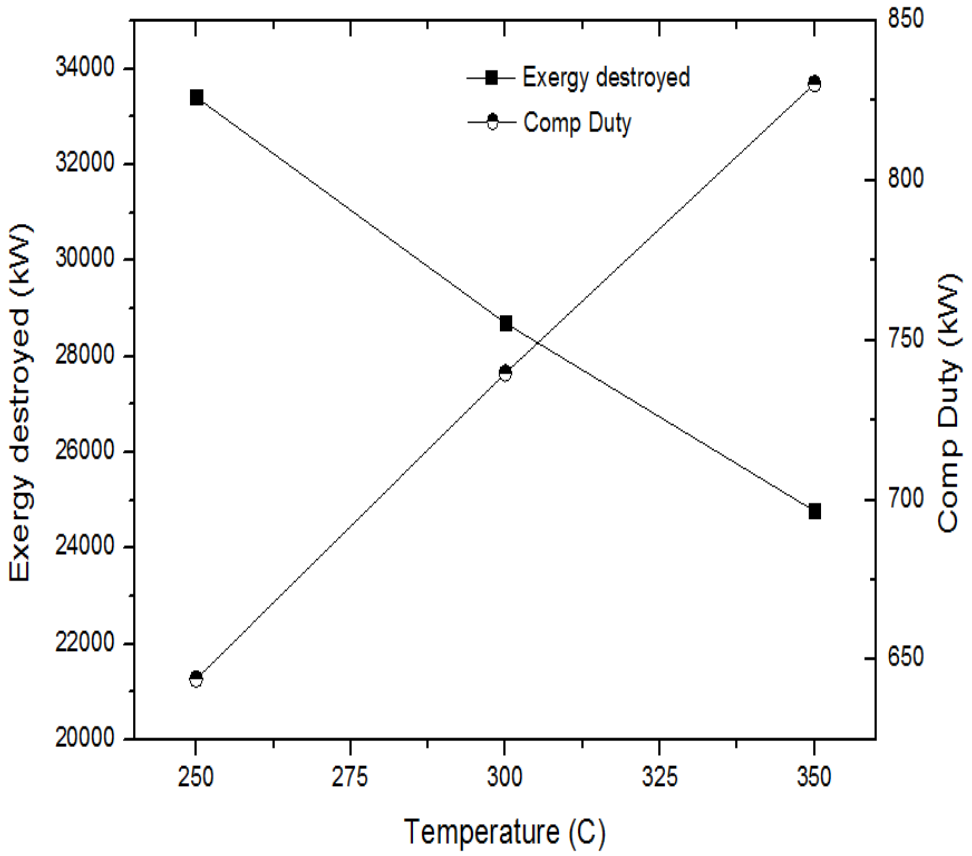

Fig. 5-10 Amount of exergy destroyed and compressor duty requirement for different temperatures

5.3.4. Economic analysis

Economic analysis was also performed to determine the optimal operating condition for the methanation process. Aspen Process Economic Analyzer (APEA V7.3.1) was used which provides an automatic linkage with the Aspen Plus simulation environment. APEA evaluates both capital (CAPEX) and operating expenses (OPEX) required for a given project by sizing the process equipments and implementing the correlations available for cost estimation. As can be seen from the technical analysis section, a significant change in compressor duty results in re-sizing of the compressor, which leads to different project CAPEX for each simulation scenario. In order to maintain the consistency in comparison, only OPEX were considered while CAPEX were assumed constant. This is reasonable because the process equipments are hardly changed during the operation of any plant whose CAPEX are determined at the early design phase. OPEX requirement with respect to change in recycle ratio is shown in Fig. 5-11. This trend is similar to that of compressor duty shown in Fig. 5-9, because electricity consumption occupies a significant portion of the OPEX for the methanation process.

For different intermediate temperatures case, the OPEX increases with increasing intermediate temperature, as shown in Fig. 5-12. At a fixed

recycle ratio value, the trend is similar but change in OPEX is not as significant as in the recycle ratio case, because the temperature has far less impact on the compressor duty compared to the flow rate.

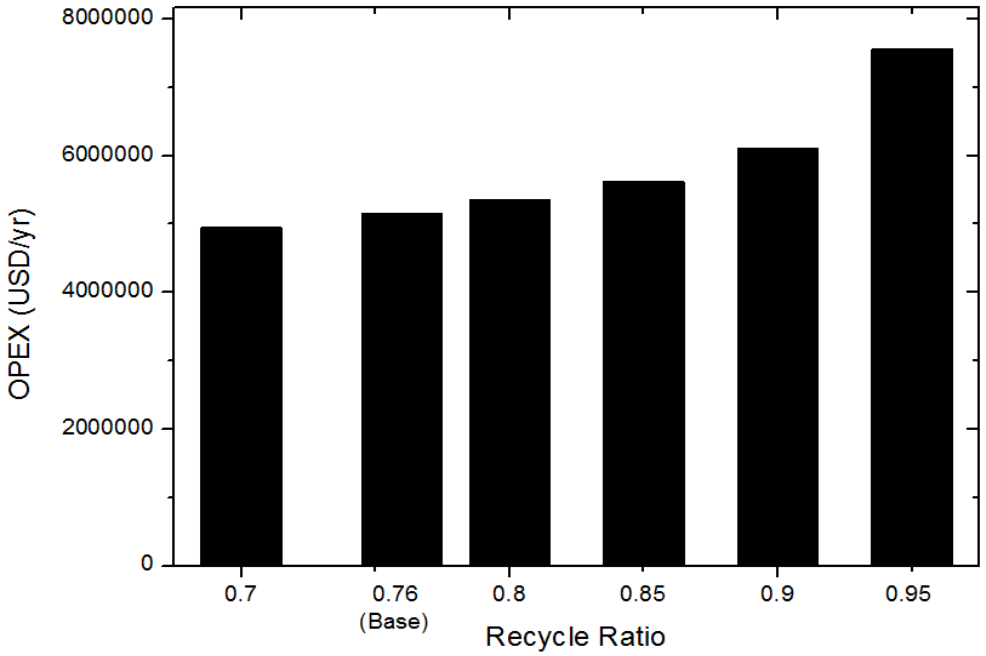

Fig. 5-11 OPEX requirement for different recycle ratio

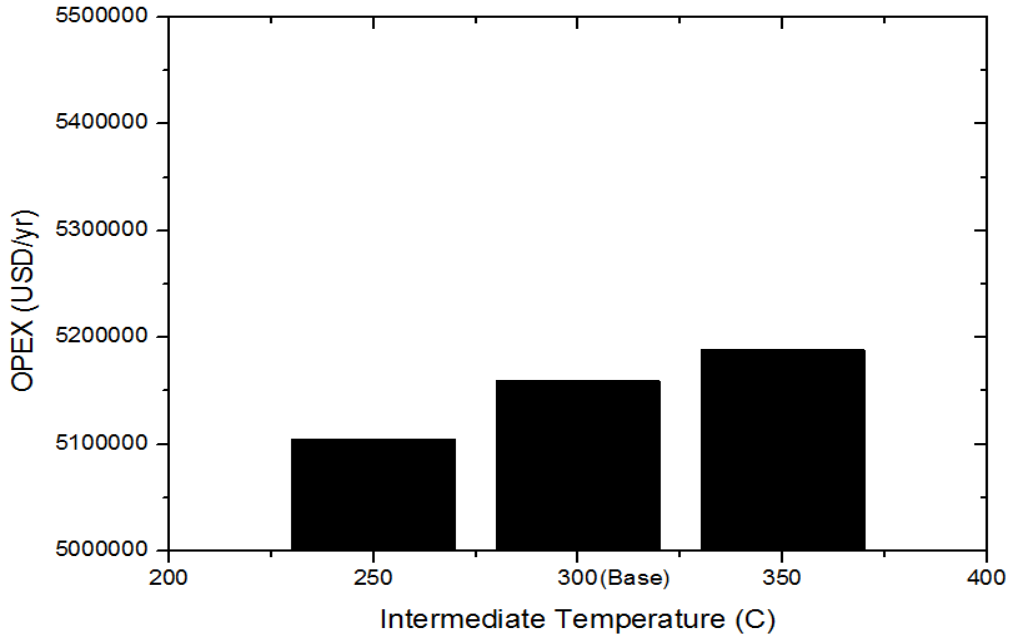

Fig. 5-12 OPEX requirement for different intermediate temperature

5.4. Results and discussion

In this chapter, methanation process for SNG production was modeled using Aspen Plus and validated against available data in the literature, and the simulation results showed reasonable agreement with the reference data. In order to determine the optimal operating condition for the methanation process, both technical and economic perspectives were considered. From technical analysis, it was found that the most of exergy loss comes from the first methanation reactor and the heat recovery following that reactor, so recycle ratio after the first reactor as well as the intermediate temperature between reactors were varied to compute the amount of exergy destroyed. At the same time, OPEX requirement was calculated using a commercial software. According to the simulation results, higher recycle ratio is favored in terms of the exergy loss. However, higher recycle ratio leads to an increase in compressor duty as well as the OPEX requirement, especially when the recycle ratio is greater than 0.9. In terms of the exergy loss, both recycle ratio and intermediate temperature have similar level of saving effect, but for the OPEX requirement, recycle ratio has much higher impact than the temperature parameter. Therefore, high recycle ratio with low intermediate temperature condition is generally favorable for the methanation process. On the other hand, one must keep in mind that at low recycle ratio and high intermediate

temperature condition, the SNG product does not meet the temperature constraints in the first reactor as well as the methane composition in the final product. Thus, these conditions must be avoided.

CHAPTER 6. Concluding Remarks

6.1. Conclusion

This thesis addressed modeling and analysis of two different CO_2 capture technologies: post-combustion and pre-combustion capture processes. Post-combustion capture can be advantageous in many aspects, especially in terms of its technical maturity, operational flexibility and expandability. However, high thermal load for solvent regeneration which leads to a reduction in power plant efficiency must be overcome to have economic feasibility for commercialization. Pre-combustion capture which can be represented by the IGCC plant, on the other hand, has a higher efficiency than conventional coal power plant. Since the CO_2 capture process is included as part of IGCC plant configuration, there is no penalty associated with capturing CO_2. Also, IGCC plant operates at relative high pressure, so physical solvents are used for acid gas removal purposes, which has significantly lower energy consumption for solvent regeneration. However, the economic barrier associated with the IGCC must be resolved in order to have feasibility for implementation.

Although the reserves of fossil fuel is rapidly diminishing, it will remain as the most dominant source for electricity generation for next few decades. If CCS policies are strictly enforced by law to reduce the

greenhouse gases, IGCC plant can also be a solution not only to capture CO_2, but also to be integrated with other renewable technologies such as SNG. It is difficult to provide quantitative criteria to determine which process type is better depending on the scenario, so for future work, rough criteria at conceptual design level will be investigated.

6.2. Future works

MVR process studied in this dissertation is currently being investigated for implementation in a large-scale CO_2 capture facility in Korea. However, the chemical solvent used in that facility is called KoSol developed by KEPCO Research Institute which has very different properties from those of MEA, so the applicability of the MVR process still remains questionable. In the future, simulation-based study to determine the MVR with different solvents can be carried out to ensure technical flexibility and compatibility of the MVR process.

For the SNG application, ideas for process intensification can be further considered. Since methanation reaction is exothermic, steam will be generated which then can be integrated with the steam turbine cycle for power generation. As licensor companies are still developing the process by changing the reaction conditions or adding heat integration schemes, there will be ample opportunities for developing process alternatives.

Literature Cited

[1] Yu C-H, Huang C-H, Tan C-S. A review of CO2 capture by absorption and adsorption. Aerosol and Air Quality Research. 2012;12:745-69.

[2] Zhu Y. Evaluation of gas turbine and gasifier-based power generation system. 2004.

[3] Mudd M. IGCC's Chasm–What Drives Technology Choices. 2003 Gasification Technologies Conference 2003.

[4] Mulder M. Basic principles of membrane technology: Springer Science & Business Media; 1996.

[5] Plaza J.M., Van Wagener D., Rochelle G.T. Modeling CO2 capture with aqueous monoethanolamine. International Journal of Greenhouse Gas Control. 2010;4:161-6.

[6] Abu-Zahra MR, Schneiders LH, Niederer JP, Feron PH, Versteeg GF. CO 2 capture from power plants: Part I. A parametric study of the technical performance based on monoethanolamine. International Journal of Greenhouse gas control. 2007;1:37-46.

[7] Takenouchi S, Kennedy GC. The binary system H 2 O-CO 2 at high temperatures and pressures. American Journal of Science. 1964;262:1055-74.

[8] Dodds W, Stutzman L, Sollami B. Carbon dioxide solubility in water. Industrial & Engineering Chemistry Chemical & Engineering Data Series. 1956;1:92-5.

[9] Drummond S.E. Boiling and mixing of hydrothermal fluids: chemical effects on mineral precipitation: Pennsylvania State University; 1981.

[10] Wang Y, Xu S, Otto F, Mather A. Solubility of N 2 O in Alkanolamines and in Mixed Solvents. The Chemical Engineering Journal. 1992;48:31-40.

[11] Austgen D.M., Rochelle G.T., Peng X, Chen C.C. Model of vapor-liquid equilibria for aqueous acid gas-alkanolamine systems using the electrolyte-NRTL equation. Industrial & Engineering Chemistry Research. 1989;28:1060-73.

[12] Hikita H, Asai S, Ishikawa H, Honda M. The kinetics of reactions of carbon dioxide with monoisopropanolamine, diglycolamine and ethylenediamine by a rapid mixing method. The Chemical Engineering Journal. 1977;14:27-30.

[13] Kucka L, Müller I, Kenig EY, Górak A. On the modelling and simulation of sour gas absorption by aqueous amine solutions. Chemical engineering science. 2003;58:3571-8.

[14] AspenTech. EAP2513.071.01. CO2 Removal Processes: Absorption using Rate-based Distillation.

[15] Hanley B, Chen CC. New mass-transfer correlations for packed towers. AIChE journal. 2012;58:132-52.

[16] Lim Y, Kim J, Jung J, Lee CS, Han C. Modeling and Simulation of CO 2 Capture Process for Coal-based Power Plant Using Amine Solvent in South Korea. Energy Procedia. 2013;37:1855-62.

[17] An J, Lee U, Jung J, Han C. Parametric optimization for power de-rate reduction in the integrated coal-fired power plant with CCS. Industrial & Engineering Chemistry Research. 2015.

[18] Alabdulkarem A, Hwang Y, Radermacher R. Energy consumption reduction in CO 2 capturing and sequestration of an LNG plant through process integration and waste heat utilization. International journal of greenhouse gas control. 2012;10:215-28.

[19] Cousins A, Wardhaugh L, Feron P. A survey of process flow sheet modifications for energy efficient CO2 capture from flue gases using chemical absorption. International Journal of Greenhouse Gas Control. 2011;5:605-19.

[20] Aly NH, El-Figi AK. Mechanical vapor compression desalination systems—a case study. Desalination. 2003;158:143-50.

[21] Liang L, Han D, Ma R, Peng T. Treatment of high-concentration wastewater using double-effect mechanical vapor recompression. Desalination. 2013;314:139-46.

[22] Bejan A. Advanced engineering thermodynamics, 1997. Wiley, New York; 1996.

[23] Yumrutaş R, Kunduz M, Kanoğlu M. Exergy analysis of vapor compression refrigeration systems. Exergy, An international journal. 2002;2:266-72.

[24] Douglas JM. Conceptual design of chemical processes1988.

[25] Rao AB, Rubin ES. A technical, economic, and environmental assessment of amine-based CO2 capture technology for power plant greenhouse gas control. Environmental science & technology. 2002;36:4467-75.

[26] Timmerhaus KD, Peters MS, West R. Plant design and economics for chemical engineers. Chemical Engineering Series. 1991.

[27] Decarre S, Berthiaud J, Butin N, Guillaume-Combecave J-L. CO 2 maritime transportation. International Journal of Greenhouse Gas Control. 2010;4:857-64.

[28] Seider WD, Seader JD, Lewin DR. PRODUCT & PROCESS DESIGN PRINCIPLES: SYNTHESIS, ANALYSIS AND EVALUATION, (With CD): John Wiley & Sons; 2009.

[29] Lee U, Yang S, Jeong YS, Lim Y, Lee CS, Han C. Carbon dioxide liquefaction process for ship transportation. Industrial & Engineering Chemistry Research. 2012;51:15122-31.

[30] Bartone L, White J. Industrial size gasification for syngas, substitute natural gas and power production. US Department of Energy, National Energy Technology Laboratory, Morgantown, WV, Paper No DOE/NETL-401/040607. 2007.

[31] Gray D, Plunkett J, Salerno S, White C, Tomlinson G. Current and Future IGCC Technologies—A Pathway Study Focused on Non-Carbon Capture Advanced Power Systems R&D Using Bituminous Coal–. DOE/NETL-2008/1337, National Energy Technology Laboratory (NETL), Pittsburgh; 2008.

[32] Gray D, Salerno S, Tomlinson G. Current and future IGCC technologies: bituminous coal to power. Falls Church (VA), USA: Mitretek (MTK). 2004.

[33] Marion C, Slater W. World Petroleum Conf., 6th. Paper; 1963.

[34] Jones D, Bhattacharyya D, Turton R, Zitney SE. Optimal design and integration of an air separation unit (ASU) for an integrated gasification combined cycle (IGCC) power plant with CO 2 capture. Fuel Processing Technology. 2011;92:1685-95.

[35] Smith A, Klosek J. A review of air separation technologies and their integration with energy conversion processes. Fuel Processing Technology. 2001;70:115-34.

[36] Newsome DS. The water-gas shift reaction. Catalysis Reviews Science and Engineering. 1980;21:275-318.

[37] Kanniche M, Bouallou C. CO 2 capture study in advanced integrated gasification combined cycle. Applied Thermal Engineering. 2007;27:2693-702.

[38] Higman C, Van der Burgt M. Gasification: Gulf professional publishing; 2011.

[39] Nannan NR, De Servi CM, van der Stelt T, Colonna P, Bardow A. An equation of state based on PC-SAFT for physical solvents composed of polyethylene glycol dimethylethers. Industrial & Engineering Chemistry Research. 2013;52:18401-12.

[40] Haar L, Gallagher JS, Kell GS. NBS/NRC steam tables: Thermodynamic and transport properties and computer programs for vapor and liquid states of water in SI units, 320 p. Hemisphere, Washington, DC. 1984.

[41] Fernandez ES, Bergsma EJ, de Miguel Mercader F, Goetheer EL, Vlugt TJ. Optimisation of lean vapour compression (LVC) as an option for post-combustion CO 2 capture: Net present value maximisation. International Journal of Greenhouse Gas Control. 2012;11:S114-S21.

[42] Jassim MS, Rochelle GT. Innovative absorber/stripper configurations for CO2 capture by aqueous monoethanolamine. Industrial & Engineering Chemistry Research. 2006;45:2465-72.

[43] Karimi M, Hillestad M, Svendsen HF. Investigation of the dynamic behavior of different stripper configurations for post-combustion CO 2 capture. International journal of greenhouse gas control. 2012;7:230-9.

[44] Le Moullec Y, Kanniche M. Screening of flowsheet modifications for an efficient monoethanolamine (MEA) based post-combustion CO 2 capture. International journal of greenhouse gas control. 2011;5:727-40.

[45] Jung J., Jeong Y. S., Lee U., Lim Y., Han C. New Configuration of the CO2 Capture Process Using Aqueous Monoethanolamine for Coal-Fired Power Plants. Industrial & Engineering Chemistry Research. 2015;54:3865-78.

[46] Association WC. The coal resources: a comprehensive overview of coal. London, worldcoal org/resources/wca-publications. 2005.

[47] Karellas S, Panopoulos K, Panousis G, Rigas A, Karl J, Kakaras E. An evaluation of substitute natural gas production from different coal gasification processes based on modeling. Energy. 2012;45:183-94.

[48] Koytsoumpa E-I, Atsonios K, Panopoulos K, Karellas S, Kakaras E, Karl J. Modelling and assessment of acid gas removal processes in coal-derived SNG production. Applied Thermal Engineering. 2015;74:128-35.

[49] Bader A, Bauersfeld S, Brunhuber C, Pardemann R, Meyer B, Siemens A, et al. Modelling of a chemical reactor for simulation of a methanisation plant. Proceedings of the 8th International Modelica Conference, Dresden, Germany2011.

[50] Er-rbib H, Bouallou C. Modeling and simulation of CO methanation process for renewable electricity storage. Energy. 2014;75:81-8.

[51] Lwin Y. Chemical equilibrium by Gibbs energy minimization on spreadsheets. International Journal of Engineering Education. 2000;16:335-9.

[52] Yu B-Y, Chien I-L. Design and Economic Evaluation of a Coal-to-Synthetic Natural Gas Process. Industrial & Engineering Chemistry Research. 2015;54:2339-52.

[53] Li S, Ji X, Zhang X, Gao L, Jin H. Coal to SNG: Technical progress, modeling and system optimization through exergy analysis. Applied Energy. 2014;136:98-109.

[54] Panek J, Grasser J. Practical experience gained during the first twenty years of operation of the great plains gasification plant and implications for

future projects. US Department of Energy-Office of Fossil Energy, Washington. 2006.

[55] Querol E, Gonzalez-Regueral B, Perez-Benedito JL. Practical approach to exergy and thermoeconomic analyses of industrial processes: Springer Science & Business Media; 2012.

[56] Jeong Y. S., Jung J., Lee U., Yang C., Han C. Techno-economic analysis of mechanical vapor recompression for process integration of post-combustion CO2 capture with downstream compression. Chemical Engineering Research and Design. 2015;104:247-55.

Abstract in Korean (요 약)

대기중으로 배출되는 온실가스 배출이 범세계적인 문제로 대두되는 기후변화에 직접적인 영향을 미치는 사실이 자명해짐에 따라 이산화탄소 포집 및 저장기술 (Carbon Capture and Storage: CCS)이 전도유망한 해결책으로 주목을 받고 있다. 이 기술은 발전소 및 철강산업에서 대량으로 배출되는 이산화탄소를 포집하여 이를 지중 혹은 해양 등 안전하게 저장 가능한 곳에 저장하는 일련의 기술을 일컫는다. CCS 기술 중에서도 포집공정의 경우 전체 에너지 사용량의 총 60-70%에 해당하는 중요한 공정으로써 상용화를 위해 공정의 최적화 및 경제성의 제고가 시급한 실정이다. 포집공정 중 연소 후 및 연소 전 포집기술은 가장 대표적으로 사용되고 있는 기술로써 전세계적으로 다양한 연구와 실증 프로젝트가 활발하게 진행되고 있다. 연소 후 포집공정은 기술적 완성도가 높고 기존 발전소와의 연계가 용이하기 때문에 상용화에 가장 근접한 기술로 평가되고 있으나 흡수제의 재생에 필요한 에너지 사용량이 높고 이는 발전소의 발전효율 감소를 초래하기 때문에 추가적인 연구가 진행되고 있다. 반면 연소 전 포집공정의 경우 상대적으로 높은 발전효율과 환경적인 측면에서 우위에 있으나 새로운 발전소의 건설이 필수적이므로 초기투자비용에 대한 단점을 지니고 있다.

본 연구에서는 석탄화력발전소의 배가스를 대상으로 모노에탄올아민 (MEA) 흡수제를 이용한 연소 후 이산화탄소 포집공정 및 대표적인 연소 전 이산화탄소 포집공정에 해당하는 석탄가스화복합발전 (Integrated Gasification Combined Cycle: IGCC) 플랜트를 각각 모델링 하고 에너지 사용량 절감을 위한 공정 개선안 및 공정의 활용 방안을 제안하고자 한다. 연소 후 포집공정은 보령화력발전소에 설치된 0.1MW 급 실험설비에서 획득한 데이터를 바탕으로 모델링 및 검증을

수행 하였으며 이 공정에 기기적 증기 재압축 시스템 (Mechanical Vapor Recompression: MVR)을 적용하여 기존 운전 대비 약 8.4%의 에너지 사용량을 절감함과 동시에 경제성 평가를 통해 개선된 운전조건을 도출하였다. 또한 실제 설비 운전시에 발생할 수 있는 기기설비적인 제한사항을 고려하여 설계 시 반드시 고려되어야 하는 가이드라인을 제시하고 있다. MVR 시스템의 경우 현재 격상 예정인 상용화급 이산화탄소 포집설비에 적용되기 위해 기술적으로 검토 중에 있으며 MEA 를 기반으로 수행된 본 연구가 향후 설계 시점에서 활용될 수 있을 것으로 판단된다. IGCC 플랜트의 경우 각 단위공정을 선진 설계사에서 취득한 공정자료를 기반으로 모델링 하였으며 발전사이클의 경우 국내 최초로 건설된 태안의 300MW IGCC 플랜트 초기 설계자료를 기반으로 모델링하였다. IGCC 플랜트의 단위공정 중 하나인 산성가스제거공정에 연소 후 포집공정에서 널리 사용되는 Lean Vapor Compression (LVC) 시스템을 적용하여 플랜트 내에서 사용되는 스팀의 사용량을 획기적으로 절감할 수 있음을 확인하였다. 또한 IGCC 플랜트에서 메탄화반응공정이 추가된 유사한 공정인 합성가스 (Synthetic Natural Gas: SNG) 생산공정을 모델링 하고 엑서지 분석 및 경제성 평가를 통해 최적의 운전조건을 도출하였다.

주요어: 연소 후 이산화탄소 포집, 연소 전 이산화탄소 포집, 모델링, 공정 개선안, 석탄가스화복합발전, 합성천연가스

학번: 2010-31329

성명: 정 영 수